Université d'Ottawa • University of Ottawa

PERMISSION DE REPRODUIRE ET DE DISTRIBUER LA THÈSE

PERMISSION TO REPRODUCE AND DISTRIBUTE THE THESIS

NOM DE L'AUTEUR / NAME OF AUTHOR:	Nilesh Patel
ADRESSE POSTALE / MAILING ADDRESS:	808-1917 St-Laurent Bld Ottawa, Ontario K1G 3S6
GRADE / DEGREE:	**ANNÉE D'OBTENTION / YEAR GRANTED**
Master of Applied Science - Chemical Engineering	2003
TITRE DE LA THÈSE / TITLE OF THESIS: Study of the Oxygen Mass Tranfer in Viscous Fermentation Systems	

L'auteur permet, par la présente, la consultation et le prêt de cette thèse en conformité avec les règlements établis par le bibliothécaire en chef de l'Université d'Ottawa. L'auteur autorise aussi l'Université d'Ottawa, ses successeurs et cessionnaires, à reproduire cet exemplaire par photograhie ou photocopie pour fins de prêt ou de vente au prix coûtant aux bibliothèques ou aux chercheurs qui en feront la demande.

Les droits de publication par tout autre moyen et pour vente au public demeureront la propriété de l'auteur de la thèse sous réserve des règlements de l'Université d'Ottawa en matière de publication de thèses.

The author hereby permits the consultation and the lending of this thesis pursuant to the regulations established by the Chief Librarian of the University of Ottawa. The author also authorizes the University of Ottawa, its successors and assignees, to make reproductions of this copy by photographic means or by photocopying and to lend or sell such reproductions at cost to libraries and to scholars requesting them.

The right to publish the thesis by other means and to sell it to the public is reserved to the author, subject to the regulations of the University of Ottawa governing the publication of theses.

N.B. LE MASCULIN COMPREND ÉGALEMENT LE FÉMININ

May 09- 2003 — Patel

DATE (AUTEUR) SIGNATURE (AUTHOR)

Université d'Ottawa · University of Ottawa

Université d'Ottawa · University of Ottawa

FACULTÉ DES ÉTUDES SUPÉRIEURES ET POSTDOCTORALES

FACULTY OF GRADUATE AND POSTDOCTORAL STUDIES

PATEL, Nilesh

AUTEUR DE LA THÈSE - AUTHOR OF THESIS

M.A.Sc. (Chemical Engineering)

GRADE - DEGREE

Chemical Engineering

FACULTÉ, ÉCOLE, DÉPARTEMENT - FACULTY, SCHOOL, DEPARTMENT

TITRE DE LA THÈSE - TITLE OF THE THESIS

Study of the Oxygen Mass Transfer in Viscous Fermentation Systems

Jules Thibault

DIRECTEUR DE LA THÈSE - THESIS SUPERVISOR

EXAMINATEURS DE LA THÈSE - THESIS EXAMINERS

A. Tremblay

A. Macchi

J.-M. De Koninck, Ph.D.

LE DOYEN DE LA FACULTÉ DES ÉTUDES SUPÉRIEURES ET POSTDOCTORALES

SIGNATURE

DEAN OF THE FACULTY OF GRADUATE AND POSTDOCTORAL STUDIES

STUDY OF THE OXYGEN MASS TRANSFER IN VISCOUS FERMENTATION SYSTEMS

By

Nilesh Patel

A thesis submitted to the Faculty of Graduate and Postdoctoral Studies in partial fulfillment of the requirement for the degree of

Master of Applied Science

In

Department of Chemical Engineering

UNIVERSITY OF OTTAWA

ABSTRACT

During aerobic fermentations, availability of oxygen to microorganisms is a very important factor for their growth and subsequent product formation. To evaluate the amount of oxygen that is available to microorganisms for their consumption, the oxygen mass transfer coefficient (K_La) is often used in the design and comparison of bioreactors. It becomes more difficult to characterize oxygen mass transfer and to design bioreactors when the viscosity of the medium constantly increases during the fermentation process. Therefore, this work is concerned with the study of K_La in viscous fermentation systems. Two types of bioreactors, the reciprocating plate bioreactor and the stirred tank bioreactor, were used to study the growth of *Aspergillus niger* and the production of citric acid. This fermentation leads to a very viscous fermentation medium due to the long filamentous structure of *Aspergillus niger*.

Before conducting fermentation experiments with the microorganism *Aspergillus niger*, wood pulp solutions were used as a model fluid to mimic its physical characteristics and to study the oxygen mass transfer in such mixtures. Experiments were done with different pulp concentrations and K_La was estimated using the gassing-out method. The estimated K_La values were then correlated to the power input per unit volume and the gas superficial velocity using a power law equation.

Fermentation experiments with *Aspergillus niger* were conducted with both bioreactors at different agitation speeds, and K_La was estimated using a data reconciliation algorithm that used 12 measured process variables and 4 mass conservation models. K_La was obtained at different stages of fermentation and at different agitation intensities. It is believed that the data reconciliation algorithm allowed reliable estimates of K_La.

RÉSUMÉ

Lors de fermentations aérobies, la disponibilité de l'oxygène pour les microorganismes est un élément très important pour sa croissance et ultérieurement pour la formation des produits. Pour évaluer la quantité d'oxygène disponible aux microorganismes pour leur consommation, le coefficient de transfert d'oxygène (K_La) est souvent utilisé pour concevoir et comparer les bioréacteurs. Il est difficile de caractériser le transfert d'oxygène et de concevoir des bioréacteurs lorsque la viscosité du milieu de fermentation augmente durant le procédé.

Ainsi, ce travail a pour but d'étudier le changement du K_La durant une fermentation dont la viscosité change constamment. Deux types de bioréacteurs, le bioréacteur à plateaux à mouvements alternatifs et le bioréacteur bien mélangé, ont été utilisés pour étudier la croissance du microorganisme *Aspergillus niger* et de la production de l'acide citrique. Cette fermentation conduit à un milieu très visqueux étant donné la nature filamenteuse du microorganisme.

Avant d'effectuer des expériences avec le microorganisme *Aspergillus niger*, des solutions de pâtes à bois furent utilisées comme fluide modèle pour imiter ses caractéristiques physiques et pour évaluer le coefficient de transfert de matière dans de tels mélanges. Des expériences furent conduites avec des solutions de concentrations différentes et le K_La fut évalué par la méthode de dégazage. Les valeurs du K_La furent corrélées à la puissance de mélange et au débit de gaz à l'aide d'une équation de la loi de puissance.

Des expériences de fermentation avec *Aspergillus niger* ont été effectuées dans les deux bioréacteurs à différentes vitesses d'agitation, et le K_La fut évalué à l'aide d'un algorithme de réconciliation des données utilisant 12 mesures de procédé et 4 équations de conservation de la matière. Le K_La a été obtenu à différents moments au cours de la fermentation et pour diverses vitesses d'agitation. Cette méthode fournit des valeurs fiables de K_La.

Statement of Contributions of Collaborators

I hereby declare that I am the sole author of this thesis. I have performed the experimental design, all experiments and the associated data analysis.

My supervisor, Dr. Jules Thibault, provided continual guidance throughout this work and made editorial comments and corrections to my written work.

Julie Goudreault and Shohini Bagchee worked as summer students in 2001. They helped in setting up the laboratory and conducting the earlier experiments. They are coauthors of the first paper.

Signature: Patel

Date: May 09-2003

ACKNOWLEDGEMENT

Many people have contributed to my thesis. First and foremost I would like to thank my supervisor, Dr. Jules Thibault, for his supervision and giving valuable suggestions and criticism throughout my research.

I would like to thank Dr. Zdravko Duvnjak for allowing me to use his research lab to perform some of my experiments. I would also like to thank Julie Goudreault, Shohini Bagchee, Sriram Kumarappan and Julie Wijaya for their support and help during my research work.

I am grateful to our department technicians, Louis Tremblay, Franco Ziraldo and Gerard Nina for their technical help in successfully running my experiments. I would like to thank the other professors and support staff, as well as the Department of Chemical Engineering for their help during my Master's study.

Finally, I would like to express my grateful thanks to my family and friends. Without their support, this work would not have been possible.

TABLE OF CONTENTS

ABSTRACT i

RÉSUMÉ ii

STATEMENT OF CONTRIBUTIONS OF COLLABORATORS iii

ACKNOWLEDGEMENT iv

TABLE OF CONTENTS v

LIST OF TABLES viii

LIST OF FIGURES ix

Chapter 1 INTRODUCTION 1

1.1 Structure of thesis 4

1.2 Reference 5

Chapter 2 WOOD PULP AS MODEL FLUID TO STUDY THE OXYGEN MASS TRANSFER COEFFICIENT IN *Aspergillus niger* FERMENTATION 6

2.1 Introduction 7

2.2 Materials and methods 10

2.2.1 RECIPROCATING PLATE BIOREACTOR (RPB) 11

2.2.2 STIRRED TANK BIOREACTOR (STB) 12

2.2.3 EXPERIMENTAL PROCEDURE 13

2.3 Theoretical background 14

2.3.1 AVERAGE POWER INPUT DETERMINATION 14

2.3.2 K_La MEASUREMENT 14

2.4 Results and discussion 16

2.4.1 OXYGEN MASS TRANSFER COEFFICIENT 16

2.5 Conclusion 25

2.6 Nomenclature 26

2.7 References 27

Chapter 3 EVALUATION OF OXYGEN MASS TRANSFER IN *Aspergillus niger* FERMENTATION USING DATA RECONCILIATION 30

3.1 Introduction 31

3.2 Materials and methods 32

3.2.1 RECIPROCATING PLATE BIORECTOR (RPB) 33

3.2.2 STIRRED TANK BIOREACTOR (STB) 34

3.2.3 EXPERIMENTAL PROCEDURE 35

3.3 Theoretical background 36

3.3.1 K_La MEASUREMENT 36

3.3.2 DYNAMIC METHOD 37

3.3.3 STATIONARY METHODS 38

3.3.4 DATA RECONCILIATION TECHINIQUE 40

3.4 Results and discussion 46

3.4.1 OXYGEN MASS TRANSFER COEFFICIENT 46

3.5 Conclusion 55

3.6 Nomenclature 56

3.7 References 58

Chapter 4 PRELIMINARY RESULTS PERTAINING TO *Aspergillus niger* FERMENTATION 60

4.1 Introduction 60

4.1.1 MATERIALS AND METHODS 60

4.2 Results and discussion 61

4.2.1 BIOMASS 61

4.2.2 CITRIC ACID 62

4.2.3 pH 63

4.2.4 POWER PER UNIT VOLUME 64

4.2.5 SUGAR COMPOSITON 64

4.3 Conclusion 65

4.4 References 65

Chapter 5 SUMMARY & CONCLUSION 67

5.1 Recommendations 68

5.2 Reference 69

APPENDIX 70

A.1 Experimental results with wood pulp in the STB. 70

B.1 Experimental results with wood pulp in the RPB. 71

C.1 Data reconciliation program 72

C.1.1 MAIN PROGRAM 72

C.1.2 SUBROUTINE GAUSSIEN 84

D.1 Experimental results for fermentation in the STB. 86

E.1 Experimental results for fermentation in the RPB. 88

F.1 Photographs of daily samples during fermentation experiments from the STB (200RPM) and RPB (0.25 Hz). 90

LIST OF TABLES

Table	Description	Page
2.1	Correlations obtained for both bioreactors.	19
3.1	Composition of the growth medium for *Aspergillus niger* fermentation.	36
3.2	Estimated values obtained for each process variable during a typical fermentation and estimated precision ($\pm 3\sigma$) of each variable.	45

LIST OF FIGURES

Figure	Description	Page
2.1	Schematic diagram of the RPB.	11
2.2	Schematic diagram of the STB.	12
2.3	Dissolved oxygen concentration as a function of time for water in the STB.	16
2.4	Oxygen mass transfer coefficient versus power input per unit volume for the RPB.	17
2.5	Oxygen mass transfer coefficient versus power input per unit volume for the STB.	18
2.6	Oxygen mass transfer coefficient for different pulp concentrations for the RPB.	21
2.7	Oxygen mass transfer coefficient for different pulp concentrations for the STB.	21
2.8	Experimental versus calculated oxygen mass transfer coefficients for the RPB.	23
2.9	Experimental versus calculated oxygen mass transfer coefficients for the STB.	23
2.10	Ratio of K_La obtained for the RPB and STB as a function of the power input per unit volume for water and a solution with a pulp concentration of 2.94 kg/m^3.	25
3.1	Determination of the oxygen mass transfer coefficient using the dynamic method.	37
3.2	Biomass concentration as a function of time for experiments conducted in the RPB and the STB at different agitation intensities.	47
3.3	Dissolved oxygen profiles for experiments conducted in the RPB and STB at different agitation intensities.	48

3.4 Experimental and predicted dissolved oxygen concentrations during the dynamic method (STB at 300 RPB on day 3). 49

3.5 K_La values obtained by four different methods and the final converged value as a function of time for the STB at 300 RPM. 50

3.6 K_La values obtained by four different methods and the final converged value as a function of time for the STB at 100 RPM. 52

3.7 K_La values obtained by four different methods and the final converged value as a function of time for the RPB at 0.75 Hz. 52

3.8 Plot of K_La values obtained for fermentation conducted in the RPB and STB versus biomass produced. 53

3.9 Plot of the normalized standard deviation of the estimation of K_La as a function of $Q_{O_2}X/K_La$ ratio for the different methods. 55

4.1 Citric acid produced with the experiments done in the RPB and the STB at different agitation speeds. 62

4.2 Measured pH as a function of time for experiments conducted in the RPB and the STB at different agitation intensities. 63

4.3 Power input per unit volume as a function of time for experiments conducted in the RPB and the STB at different agitation intensities. 64

4.4 Sugar concentration as a function of time for experiments conducted in the RPB and the STB at different agitation intensities. 65

CHAPTER 1

INTRODUCTION

Although most chemicals are still derived from petrochemicals, the last decades have seen a tremendous increase in bio-based products. The foreseeable depletion of petroleum and the environment-friendly aspect of bio-based products have forced the chemical industry to put more emphasis on the production of many chemicals using microorganisms. In United States, the government has targeted a three-fold increase in bio-based products by the end of the decade (Gonzales and Reicher, 2001). The Canadian Government is following along the same line and supporting Canadian industries to produce more bio-based products.

The history of fermentation goes back to the time when wine along with other food products like cheese, bread, yogurt and soy were produced. However, it is only in the 19^{th} century, due to the work of Pasteur and Tyndall, that microbiology became a science. At the beginning of the 20^{th} century, chemicals such as ethanol, citric acid and glycerol were commonly produced. During the Second World War, due to the huge demand for antibiotics such as penicillin, a new body of knowledge was created, which is known today as biochemical engineering. Better design of bioreactors and optimization of the production became an important part of biotechnology. Biotechnology has come a long way from being used to produce only food products. Today, there is a myriad of chemicals, antibiotics and steroids that are commonly produced by microorganisms.

There are certain limitations associated with manufacturing bio-based products. For example, the medium has to be kept sterile and proper nutrients have to be provided to the

microorganism for their growth. Especially during aerobic fermentation, the oxygen supply to the microorganism is critical for their growth and subsequently to the product formation. This oxygen demand can be met by increasing the oxygen concentration in the inlet gas stream but this would considerably increase the overall cost of production. Better mixing devices and more efficient bioreactors are more acceptable alternatives to this problem. There are many types of bioreactors and mixing devices used in industry. These are selected depending on the type of mixing to be achieved and on the type of microorganism. For example, during aerobic fermentation, vivid mixing is used to supply enough oxygen to the microorganisms for their growth. However, if the microorganisms are susceptible to high shear, then an optimum mixing speed and/or a low-shear mixing device have to be used in order for the microorganisms to have sufficient supply of oxygen and yet not affected by the level of shear caused by mixing device.

The problem of improper mixing becomes more severe when the viscosity of the fermentation broth increases during the fermentation process. Therefore, it becomes very difficult to design bioreactors for viscous fermentation processes. The increase in viscosity might be due to the production of a viscous product or due to the growth of viscous microorganisms. An example of an increase in viscosity due to the formation of a product is the pullulan fermentation. Audet (1996) and Thibault and LeDuy (1999) have previously studied this type of fermentation. Therefore, this thesis is concerned with the fermentation process when the increase in viscosity is due to the growth of microorganisms. One example of this type of fermentation processes, which is the subject of this thesis, is the production of citric acid using the microorganism *Aspergillus niger*. Even though the microbial production of citric acid has been widely studied, it was selected because is a good representation of the type of viscous fermentation systems that was targeted in this investigation. It was Wehmer

in 1893 (Wehmer, 1907) who first showed that certain fungi produced citric acid when grown on sugar solutions. However, it was only following the work of Curie (Curie, 1917) that the production of citric acid from *Aspergillus niger* became industrially possible. Today, most of the citric acid used in food and in various other industries is produced from submerged fungal fermentation.

Before studying the fermentation process, a model fluid consisting of wood pulp suspensions was used to characterize the oxygen mass transfer. Wood pulp was selected due to its close physical resemblance with *Aspergillus niger*. Experiments were performed with two different types of bioreactors: a reciprocating plate bioreactor (RPB), which has an axial-type mixing device and a stirred tank bioreactor (STB), which has a radial-type mixing device. In order to study the oxygen availability to the microorganism, oxygen mass transfer coefficient (K_La) is often used. The effect of power and superficial gas velocity on the oxygen mass transfer coefficient (K_La) was studied by correlating K_La with these two process variables using the power law equation.

Then, both the RPB and the STB were used for *Aspergillus niger* fermentation. K_La was estimated throughout the fermentation using data reconciliation. There exist many different methods to calculate K_La, which are broadly classified as dynamic and steady state methods. Ideally, all these methods should give identical K_La values. However, due to the errors associated with the measured variables, each method usually gives a different estimate of K_La. To obtain a more reliable and unique estimate, a data reconciliation algorithm is used. The estimated value of K_La is obtained by taking into consideration both the reliability of measured data and the accuracy of each estimation method.

1.1 Structure of thesis

The main body of this thesis consists of two papers and a chapter containing all the remaining results not included in the two papers. One paper (Chapter 2) has been submitted for publication and the other will be submitted shortly.

In Chapter 2 (first paper), wood pulp is used as a model fluid to mimic the actual fermentation process of *Aspergillus niger*. The experiments were done with the reciprocating plate and the stirred tank bioreactors for different air flow rates and agitation speeds. The oxygen mass transfer coefficient was estimated for each experimental condition and for various wood pulp concentrations. The estimated K_La values were then correlated as a function of the power input per unit volume and the gas superficial velocity using a power law equation. Correlations were obtained for different concentrations of wood pulp.

The third chapter deals with fermentation experiments done with the microorganism *Aspergillus niger* in view of measuring the oxygen mass transfer coefficient during the course of the fermentation. Four sets of experiments were done in each bioreactor and, during each experimental run, the dissolved oxygen concentration was measured online. Data reconciliation was successfully used to obtain a unique and more reliable value of the oxygen mass transfer coefficient from four different methods.

In Chapter Four, results that are not included in the other two papers are presented. These results were obtained by analyzing the samples collected everyday during fermentation experiments done with *Aspergillus niger*. The samples were analyzed for pH, biomass, citric acid and sugar concentrations.

Finally, a summary of the important findings and various conclusions drawn from this study are presented in Chapter 5 along with few recommendations. Nomenclature and

references are provided at the end of the each chapter and an appendix at the end of the thesis.

1.2 REFERENCES

Audet, J., J. Thibault and A. LeDuy, "Polysaccharide Concentration and Molecular Weight Effects on the Oxygen Mass Transfer in a Reciprocating Plate Bioreactor", Biotechnol. Bioeng. **52**, 507-517 (1996).

Currie, J., "The Citric Acid Fermentation of *Aspergillus niger*", J. Biol. Chem. **31**, 15-37 (1917).

Gonzales, M. and D. W. Reicher (Co-Chairs), "Fostering Bioeconomic Revolution in Biobased Products and Bioenergy – An Environmental Approach" Report NREL/BR-510-30185 prepared by Biomass Research and Development Board (http://www.bioproducts-bioenergy.net/existsite/pdfs/strategicplan.pdf, last accessed 31/March/2003), Jan 2001

Thibault, J and A. LeDuy, "Pullulan, Microbial Production Methods", In M.C. Flickinger and S.W. Drew, Encyclopedia of Bioprocess Biotechnology: Fermentation, Biocatalysis, and Bioseparation, John Wiley & Sons, Inc., 2232-2247 (1999).

Wehmer, C., In "Handbuch der Technischen Mykologie", F. Lafar, ed., **4**, 192 (1907).

CHAPTER 2

Wood Pulp as Model Fluid to Study the Oxygen Mass Transfer in *Aspergillus niger* Fermentation

Nilesh Patel, Julie Goudreault, Shohini Bagchee *and* Jules Thibault
Department of Chemical Engineering
University of Ottawa
Ottawa (ON), K1N 6N5, Canada

Abstract

To characterize the oxygen mass transfer in a fermentation system and to study the efficiency of mixing devices, model fluids are often used so that experimental conditions can be better controlled. In this study, wood pulp solutions were used to mimic the rheological properties of fermentation broths of *Aspergillus niger*. Two different types of bioreactors were used: a reciprocating plate bioreactor and a stirred (Rushton) tank bioreactor. The oxygen mass transfer coefficient (K_La) was measured for various mixing intensities, air flow rates and wood pulp concentrations, and a correlation of K_La as a function of the power input per unit volume and the superficial gas velocity was derived for each bioreactor and each pulp concentration. K_La was found to increase with agitation and air flow rate, and was adversely affected by an increase in pulp concentration for reciprocating plate bioreactor.

Keywords: bioreactor, fermentation, model fluids, oxygen mass transfer coefficient.

2.1 Introduction

An important goal in most aerobic fermentations is to maintain an optimal level of dissolved oxygen concentration to provide an environment to the microorganisms that is conducive to high growth and/or production rates. Often, these rates are limited by the availability of dissolved oxygen. One of the important parameters used to design bioreactors and also to estimate the availability of dissolved oxygen for microorganism consumption is the oxygen mass transfer coefficient (K_La). Because the solubility of oxygen in aqueous systems is very low, it is necessary to have a high K_La. K_La is influenced by numerous factors, the most important ones being the viscosity of the fermentation broth, the type of mixing device and the intensity of mixing.

The rheological properties of many fermentation media change during the course of the fermentation process due to the growth of microorganism and/or product formation. For example in the case of pullulan production using *Aureobasidium pullulans*, the viscosity of the fermentation broth can increase by many orders of magnitude during the course of fermentation because of the long water-soluble biopolymer chains that are synthesized (Lounes et al., 1995; Audet et al., 1996; Thibault and LeDuy, 1999). On the other hand, for filamentous microorganisms, the drastic increase in viscosity is associated with the growth and morphology of microorganisms. This is the case of *Aspergillus niger*, which forms mycelia and/or pellets (Allen, 1990). For both cases, the oxygen mass transfer coefficient is significantly reduced as the concentration of either the product or the microorganism increases with time.

To enhance the oxygen transfer rate to the fermentation medium, an oxygen-enriched gas stream can be used instead of air but it is rarely economically feasible. More practical

alternatives to increase the oxygen transfer rate reside in an increase in the volumetric oxygen transfer coefficient, K_La, using higher airflow rate, better mixing devices and/or higher mixing intensity. However, there is an economic cost associated with increasing these parameters. In addition, too vigorous agitation can subject the microorganisms to high shear stress, which can be detrimental to their growth and ability to produce the desired product especially for filamentous microorganisms. Finding an optimum operating point for these parameters therefore becomes an important issue. For highly viscous fermentation broths, the use of traditional mixing devices such as Rushton turbines leads to non-uniform K_La within the fermenter (Lounes et al., 1995). It is usually large in the vicinity of the mixing element and significantly lower further away. Due to this non-homogeneous mixing, three mixing zones have been observed: a micromixing zone in the vicinity of the impeller where mixing is vivid, a macromixing zone where the broth circulates very slowly with very little intimate mixing and a stagnant zone in the periphery of the bioreactor where the broth is motionless. In such situations, it is important to choose a mixing device that can significantly reduce or even eliminate stagnant zones while providing a better and homogeneous overall volumetric oxygen mass transfer coefficient.

Several unconventional mixing devices have been designed and studied. These are the reciprocating plate mixer (Lounes et al., 1995), the helical ribbon mixer (Jolicoeur et al., 1992), and the helical ribbon screw mixer (Tecante and Choplin, 1993). Helical ribbon mixers are good for mixing but relatively poor for oxygenation. A mixing device that appears to be particularly well suited for highly viscous fermentation is the reciprocating plate bioreactor (RPB). It consists of a stack of perforated plates mounted on a vertically reciprocating shaft to agitate the vessel contents. Lounes et al. (1995) give a detailed description of this type of bioreactors. The reciprocating plates occupy the whole cross-

sectional area of the bioreactor and, as a result, energy is imparted more gently and uniformly throughout the fermentation medium.

Because of the evolving rheological properties of these highly viscous fermentations, it is difficult to have a reliable estimation of K_La during the course of fermentation. To circumvent this problem, many authors have measured K_La for model fluids instead of fermentation broths. Fluid models such as H_2O (Baird and Rama Rao, 1998, Linek et al., 1987), aqueous solution of CMC (Popovic and Robinson, 1989), dextran (Audet et al., 1996) were chosen to mimic as closely as possible the rheological behaviour of fermentation broths at different stages of fermentation. Model fluids have the distinct advantage that they can be precisely characterized and their rheological properties remain the same during the entire experimental tests. In this paper, different concentrations of wood pulp solutions were used to mimic the rheological behaviour of the fermentation broth associated with the growth of *Aspergillus niger*. Allen and Robinson (1989) have used aqueous solution of CMC as the fluid model for the identical fermentation and were able to use results of the fluid model to gain valuable information on the fermentation. Wood pulp is heterogeneous and, with its relatively long fibers, forms a mixture that resembles closely the physical appearance and the apparent rheological behaviour of a typical fermentation of *Aspergillus niger*. In a typical fermentation, the culture medium initially exhibits Newtonian behaviour but, as the fermentation progresses, it becomes highly viscous and non-Newtonian. The consistency of the pulp mixture can easily be changed by adding larger quantity of fibers to reflect the physical appearance of the broth at different stages of the fermentation. Even though it is not always possible to directly relate results from the model fluid to actual fermentation systems, these results are nevertheless very useful to evaluate the performance of mixing devices and changes of K_La with operating conditions.

The objective of this paper is to examine the relation of gas flow rate and power input per unit volume to K_La for various wood pulp solutions. It will also be interesting to compare K_La results obtained with wood pulp solutions with those measured during citric acid fermentation by *Aspergillus niger*.

2.2 Materials and methods

The two bioreactors, a reciprocating plate bioreactor and a stirred tank bioreactor with three Rushton turbines, were used throughout these experiments. These bioreactors, built in our laboratories, are identical except for the mixing mechanism. The experimental setup is similar to one used by Gagnon et al. (1998). The two bioreactors have a total volume of 22.5 L and a working volume of 17-18 L. The bioreactors are made of stainless steel and have an inner diameter of 228 mm and a column height of 550 mm. The outer tube has an internal diameter of 236 mm that leaves an annular gap of 3.5 mm where water, at an appropriate temperature, is continuously circulated to maintain the temperature of the fermentation broth constant at 30 °C. The top of the bioreactor has ports for sampling and to hold a 19 mm dissolved oxygen probe (Ingold, Model 322756202) and a thermocouple. Compressed air or nitrogen from a cylinder is fed at the bottom of the bioreactor after passing through a rotameter, a mass flow meter (Matheson, Model 8273-0434) and a sterile gas filter. The gas sparger at the bottom of the bioreactor contains one hundred uniformly distributed holes, 1 mm in diameter. The gas flow rate is controlled by a mass flow meter and the dissolved oxygen probe measures the dissolved oxygen at a point located 82 mm from the centre of the column and 255 mm from the bottom of the bioreactor.

2.2.1 RECIPROCATING PLATE BIOREACTOR (RPB)

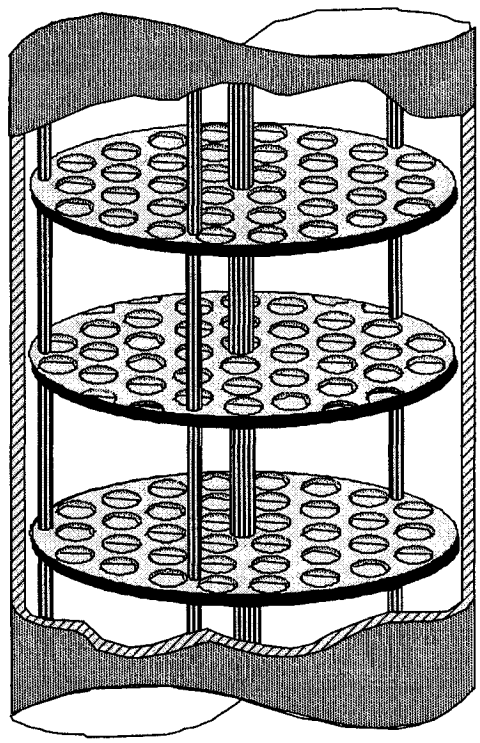

Figure 2.1 – Schematic diagram of the RPB

A schematic view of the plate stack used in the RPB is shown in Fig. 2.1. The plate stack consisted of 6 perforated stainless steel plates, 221 mm in diameter and 1.25 mm thick. Each plate was spaced 50 mm apart from one another. The perforations have a diameter of 19 mm and holes are distributed on an equilateral triangular pitch. The plate fractional free area, including the 3.5 mm annular space between the plate edge and bioreactor wall, is 0.357. The power imparted by the plate stack to fermentation medium or fluid model is calculated from variations in the pressure at the base of the column. The instantaneous pressure was measured by a pressure transducer (Cole Parmer Model H-068845-52) connected to the bottom of the bioreactor. The driving unit consists of a connecting rod, which imparts the reciprocating motion, a tenfold reducing speed transmission and a variable speed motor controlled by a microcomputer. The frequency of the reciprocation was measured using an

aluminum disc, containing 100 uniformly distributed perforations and mounted on the output shaft of the reducing transmission, used in conjunction with an infrared optical switch (HOA-2001, Honeywell). The frequency was controlled by manipulating the power to the motor.

2.2.2 STIRRED TANK BIOREACTOR (STB)

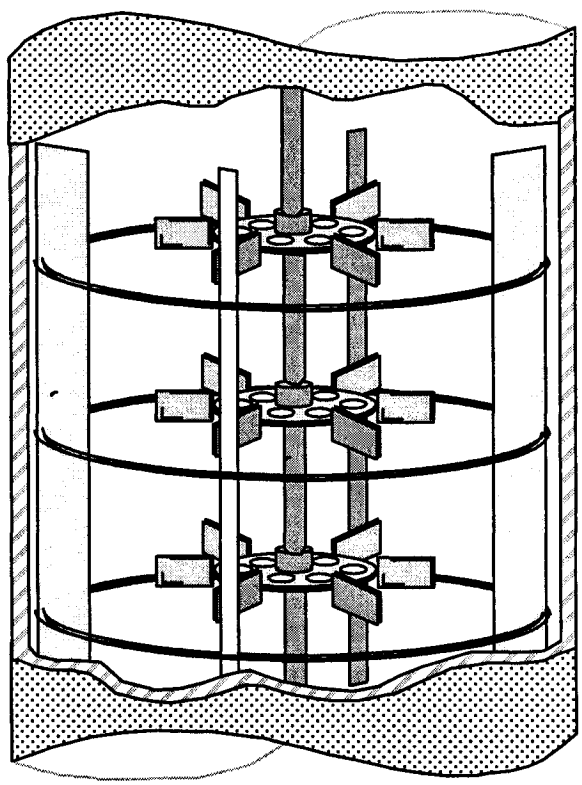

Figure 2.2 – Schematic diagram of the STB

A schematic view of the mixing device used in the stirred tank bioreactor is shown in Fig. 2.2. The three identical Rushton turbines were mounted on the central shaft. The locations of the impellers, measured from the bottom of the column, are 56, 199 and 327 mm. Each turbine has 6 blades mounted on the periphery of a 50 mm diameter disk. Each blade is 25

mm long, 15 mm high and 1.5 mm thick. Four baffles, 375 mm high, 16 mm wide and 1 mm thick, were placed inside the mixing vessel.

The impeller shaft is driven by a mechanical system composed of a motor (90 VDC, 1800 RPM, ½ HP, Frame 56C, Model 8293, Pacific-Scientific) and a ten-to-one speed reducer assembly (Model 201657, Doerr Electric). A speed controller (Multi-Drive Model KBMD-240D, KB Electronics, Inc.) connected to the motor allows a variable speed in both clockwise and counter-clockwise rotation. Torque is measured with a non-contact strain gage torquemeter (S. Himmelstein & Co., Model MCRT 24-02T, 25-0). The operating range for the torque and the speed are 0 to ±2.82 Nm and 0 to 1000 RPM, respectively. The torque and speed output signals were amplified and read on the digital display of a modular unit (S. Himmelstein & Co. System 6 recorder including a digital counter Model 6-206b, a transducer amplifier model 6-201 and scanner Model 6-405B). The recorder has an analog voltage output that allows the torque and speed to be read by a microcomputer.

2.2.3 EXPERIMENTAL PROCEDURE

The pulp used for the experiment was obtained from the final stages of a Kraft bleaching process. It was graciously donated from the Eddy Specialty Paper plant, a division of Domtar Inc., in Ottawa, Canada. The concentration of the supplied pulp was found to be 50 kg/m^3 of solution. A first set of experiments was done using distilled, deionized water, whereas the remaining tests were conducted with wood pulp concentrations of 1.47, 2.94 and 4.12 kg/m^3. The RPB was run at frequencies of 0.1, 0.25, 0.5, 0.75, 1.00 and 1.25 Hz with superficial gas velocities of 0.002, 0.0041, 0.0081, 0.0122 m s^{-1}. The STB was run at 50, 100, 200, 300 and 400 RPM with identical gas flow rates as those used in the RPB.

2.3. Theoretical background

2.3.1 AVERAGE POWER INPUT DETERMINATION

For gas-liquid contacting, the performance of a mixing device is normally assessed by its ability to provide high mass transfer coefficients with minimum power input per unit volume.

RPB system

The power input (P_G) was calculated using the method proposed by Lounes and Thibault (1993). This method uses the instantaneous pressure drop (Δ_P) at the bottom of the column:

$$P_G = A_c \left| \Delta_P V_P \right| \tag{2.1}$$

The time averaged power consumption ($\overline{P}_G$) was then determined by numerical integration of the instantaneous power consumption (P_G) over four complete periods of oscillation (4T):

$$\overline{P}_G = \frac{1}{4T} \int_0^{4T} P_G dt \tag{2.2}$$

STB system

For the stirred tank bioreactor, equipped with Rushton turbines, power input is calculated using torque (M) and rotational speed (N) as follows:

$$\overline{P}_G = C(M - M_0)N \tag{2.3}$$

M_0 is the torque required to rotate turbines in air (empty column).

2.3.2 K_La MEASUREMENT

The overall oxygen mass transfer coefficient was determined using the gassing-out method (Lounes and Thibault, 1993). A stream of nitrogen gas was first passed through the bioreactor to completely purge any dissolved oxygen. Then, gas flow rate was switched to air

and the dissolved oxygen concentration was read until saturation was reached. This procedure was followed for all different combinations of agitation and gas flow rates for different pulp concentrations.

K_La was estimated with the data obtained during the gassing-out method. Oxygen mass transfer from gas phase to the probe, where it is detected, can be divided into three transport resistances:

Gas Phase

$$\varepsilon \frac{\partial C_G}{\partial t} = U_G \frac{\partial C_G}{\partial z} - K_L a\left(C_L^* - C_L\right) \tag{2.4}$$

Liquid Phase

$$\frac{\partial C_L}{\partial t} = K_L a\left(C_L^* - C_L\right) \tag{2.5}$$

Probe Dynamics

$$\tau_P \frac{dC_P}{dt} = C_L - C_P \tag{2.6}$$

Probe dynamics also includes the resistance of the stagnant film. These three equations were solved simultaneously by finite differences with the use of a nonlinear regression program to obtain an estimated K_La that minimizes the sum of squares of the residuals between the experimental and predicted dissolved oxygen concentrations. A typical plot of the experimental and predicted dissolved oxygen concentration as a function of time is presented in Fig. 2.3.

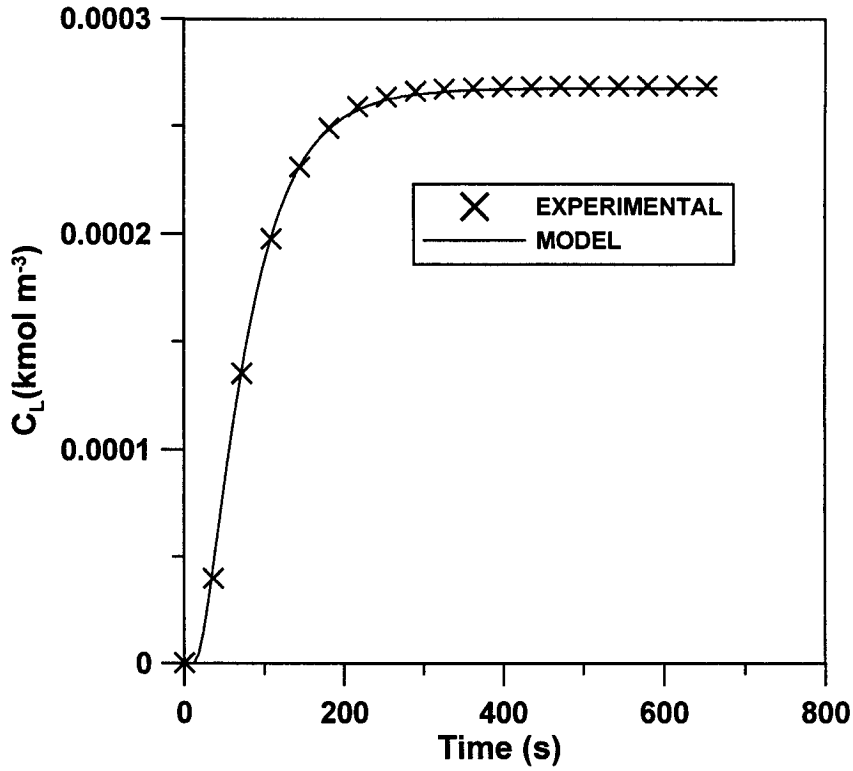

Figure 2.3 – Dissolved oxygen concentration as a function of time for water in the STB.

2.4 Results and discussion

2.4.1 OXYGEN MASS TRANSFER COEFFICIENT

Choosing a mixing device for a particular aerobic fermentation is a considerable challenge. It is desirable to have a high and uniform oxygen mass transfer coefficient throughout the bioreactor with minimum energy requirements. This is a very important consideration since the solubility of oxygen is very low and often a limiting factor for greater productivity. The oxygen mass transfer coefficient depends on several factors such as the geometry of the bioreactor, fluid rheology and operating conditions. It has traditionally been observed that K_La increases with superficial gas velocity and with power input per unit volume. This dependence has commonly been reported using the following relationship:

$$K_L a = \gamma\left(\overline{P_G}/V_L\right)^{\alpha} U_G^{\beta} \tag{2.7}$$

Sometimes, additional terms are added to include the effect of the apparent viscosity of the medium. Different values of the coefficients α, β and γ have been found by different authors (Bailey and Ollis, 1986) depending on the type of bioreactor, agitation used and the nature of the medium.

Equation (2.7) was used in this investigation to encapsulate variations in the oxygen mass transfer coefficient ($K_L a$) as a function of the power input per unit volume and the gas superficial velocity for water and the three wood pulp concentrations. Fig. 2.4 and 2.5 present the variation of $K_L a$ for a wood pulp concentration of 2.94 kg/m^3 for the reciprocating and stirred tank bioreactors, respectively. As observed in these graphs, the general trend for the variation of $K_L a$ is similar for both mixing devices. There are two distinct regimes of operation. For low values of power input per unit volume, the oxygen

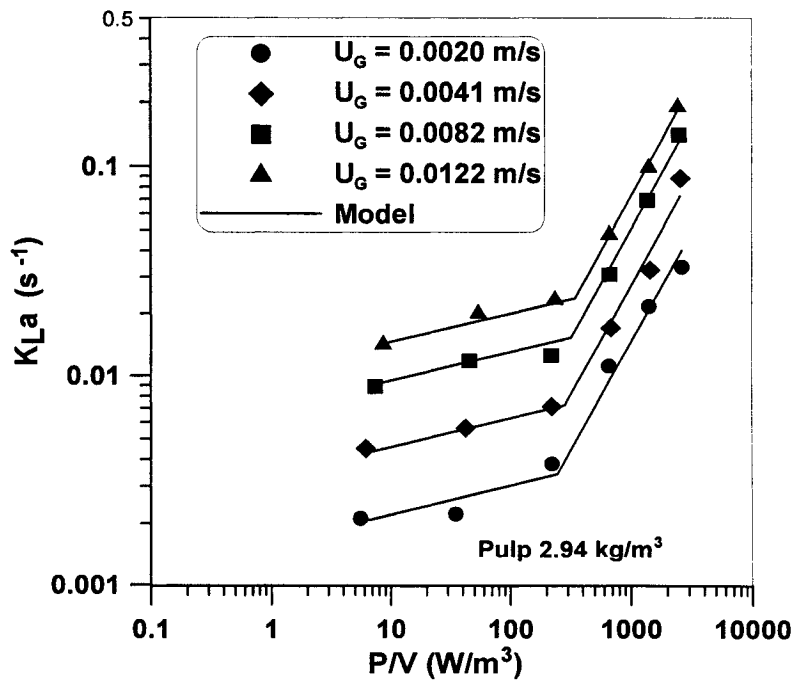

Figure 2.4 – Oxygen mass transfer coefficient versus power input per unit volume for the RPB.

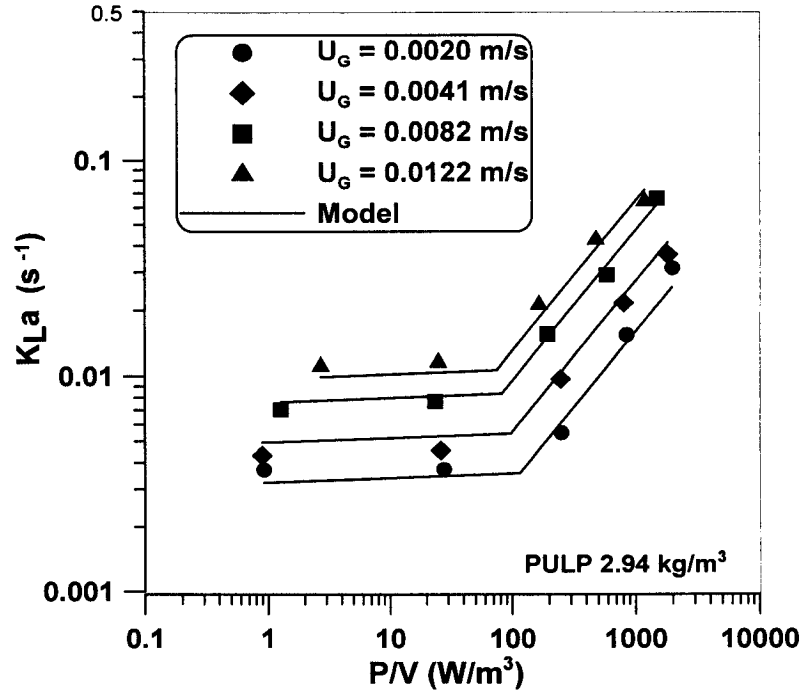

Figure 2.5 – Oxygen mass transfer coefficient versus power input per unit volume for the STB.

mass transfer coefficient is a very weak function of the power input per unit volume whereas it varies considerably with the superficial gas velocity. At lower agitation speeds, energy given to the gas-liquid mixture is not intense enough to break gas bubbles and, as a result, increase the volumetric surface area (a). Above a certain threshold of power input per unit volume, approximately 250 W/m^3 for the RPB and 90 W/m^3 for the STB, there is a significant increase of K_La with power input per unit volume. Previous works by Gagnon et al., (1998), Perez and Sandall (1974) and Nishikawa et al. (1981) have all observed two distinct regimes of operation. The threshold power per unit volume is lower for the STB than for the RPB because power imparted to the fluid is highly concentrated at the tips of the impeller blades, thereby creating zones of high shear rate that can rupture gas bubbles, whereas in the RPB, power is more uniformly distributed. Increasing the intensity of agitation results in the production of smaller bubbles that have greater probability of being

retained for a longer period of time in the bioreactor and thereby leading to an increase in gas holdup. Lounes et al. (1995) have clearly shown that the gas holdup as a function of power input per unit volume also had two distinct regimes and similar threshold values were obtained.

Table 2.1 - Correlations obtained for both bioreactors

Reciprocating Plate Bioreactor			
Conc. kg/m^3	**γ**	**α**	**β**
REGIME I			
0.00	0.577	0.204	0.921
1.47	0.852	0.094	0.983
2.94	1.114	0.137	1.056
4.12	0.565	0.076	0.934
REGIME II			
0.00	0.0045	1.294	1.197
1.47	0.0007	1.322	1.011
2.94	0.0027	1.045	0.891
4.12	0.0006	1.208	0.908
Stirred Tank Bioreactor			
REGIME I			
0.00	0.577	0.061	0.946
1.47	0.181	0.051	0.688
2.94	0.147	0.022	0.616
4.12	0.147	0.042	0.629
REGIME II			
0.00	0.0076	0.658	0.551
1.47	0.0200	0.665	0.792
2.94	0.0164	0.692	0.777
4.12	0.0145	0.703	0.783

The different values of the parameters of Equation (2.7) are given in Table 2.1 for the two bioreactors and for the four liquid solutions. In the first regime, there is little influence of the increase in power input per unit volume on K_La, which is clearly shown by the low average exponent value of the power input per unit volume term of Equation (2.7). This influence is nevertheless larger for the RPB, mainly because the plates prevent gas bubbles from rising rapidly through the liquid column to the surface. For both bioreactors, exponent α slightly decreases as the pulp concentration increases. The main contribution to the increase of K_La in the first regime is the superficial gas velocity. In the first regime, the two bioreactors are akin to a simple gas column.

Shifting to the second regime, the exponent values of the superficial gas velocity remain nearly constant to those observed in the first regime. On the other hand, the exponent values of power input per unit volume increase drastically. As discussed previously, beyond a critical threshold of power input per unit volume, the influence of power input per unit volume on K_La is much stronger. The reciprocating plate bioreactor gave higher K_La and better utilization of the power imparted to the fluid to promote gas-liquid contact. In the RPB, mixing is more uniform because the moving plate occupies the total cross-section of the column. For the RPB, exponent α is nearly twice the value obtained for the STB, resulting in a more efficient utilization of the energy imparted to the mixing device.

Plots of K_La versus pulp concentration are shown in Fig.2 6 and 2.7 for the RPB and STB, respectively. It is interesting to note that K_La decreased with increasing pulp concentration for the RPB whereas it remained relatively constant for the STB. The results of the RPB were expected since the fraction of power input per unit volume actually used to break the

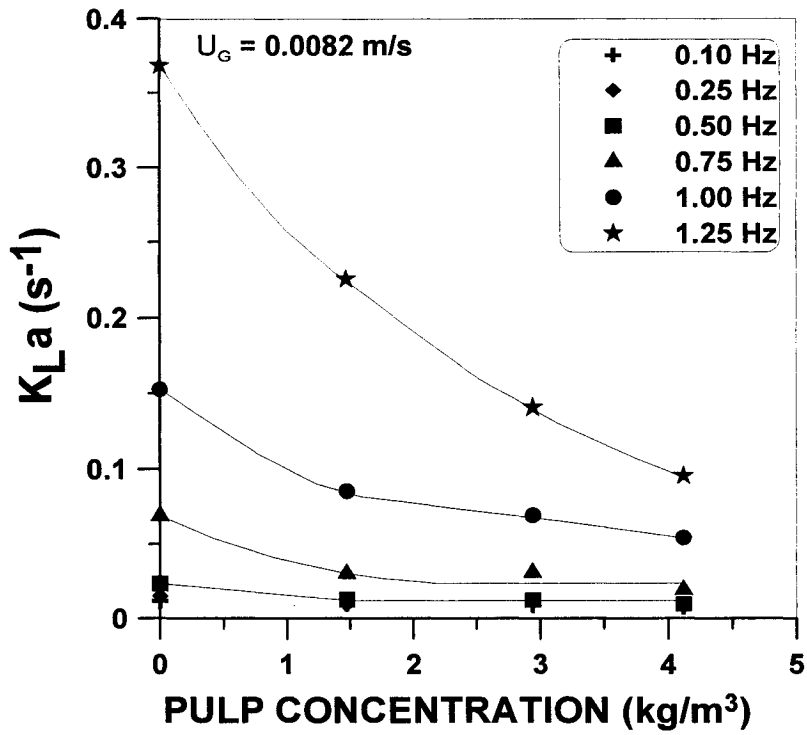

Figure 2.6 – Oxygen mass transfer coefficient for different pulp concentrations for the RPB.

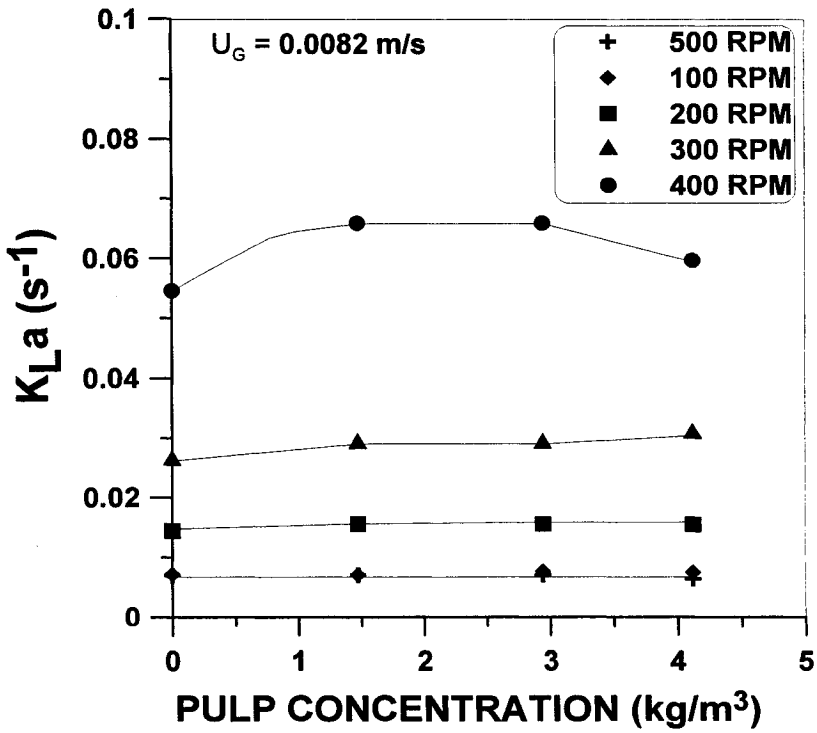

Figure 2.7 – Oxygen mass transfer coefficient for different pulp concentrations for the STB.

gas bubbles is reduced as the concentration of pulp is increased. The reason for the atypical behavior observed in the STB is due to the localized mixing achieved with the Rushton turbine mixing system and to the characteristics of wood pulp solutions. Pulp fibers in solution, subjected to a centrifugal force induced by the rotating Rushton turbines, have a tendency to concentrate more heavily in the outer zone of the bioreactor. The dissolved oxygen probe was located 82 mm from the center of the 228 mm diameter column. Therefore the probe was located in a region of wood pulp concentrations lower than if the pulp would have been uniformly mixed. For the same reason, it was not possible to determine the viscosity of pulp solutions with conventional viscometers. On the other hand, due to the uniform mixing achieved in case of the RPB, a significant decrease in K_La with increasing pulp concentration was observed. This clearly shows that the RPB is a more appropriate mixing device than the STB for this type of fluids. Due to the non-homogeneous pulp concentration in the STB, a wood pulp solution is not an ideal model fluid for this type of bioreactors. Nevertheless, it provides some tendencies in the variation of K_La with the main operating variables.

Fig. 2.8 and 2.9 show parity plots between the experimental and predicted oxygen mass transfer coefficients (using the parameters of Equation (2.7) and Table 2.1) for the two bioreactors. The plots clearly show that all correlations are a sufficiently good representation of the experimental data and can be used with confidence.

Fig. 2.10 presents two plots of the ratio of the oxygen mass transfer coefficient in the RPB to the one in the STB as a function of the power input per unit volume. The general trend observed in the graphs of Fig 2.10 was obtained for water and all wood pulp concentrations. The K_La ratio initially increases with the power input per unit volume up to the power threshold of the STB and then decreases until the power threshold of the RPB is reached.

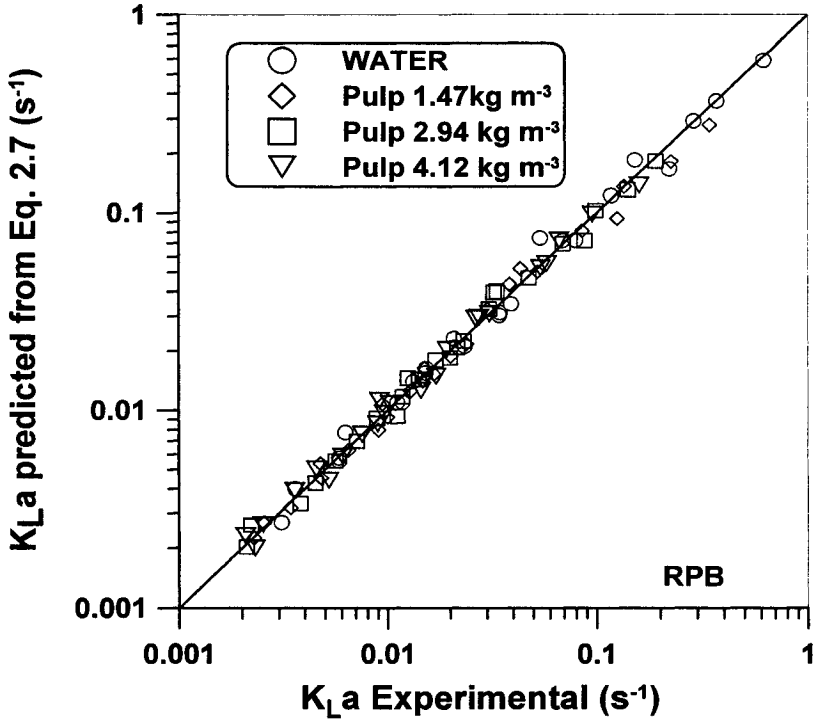

Figure 2.8 – Experimental versus calculated oxygen mass transfer coefficient for the RPB.

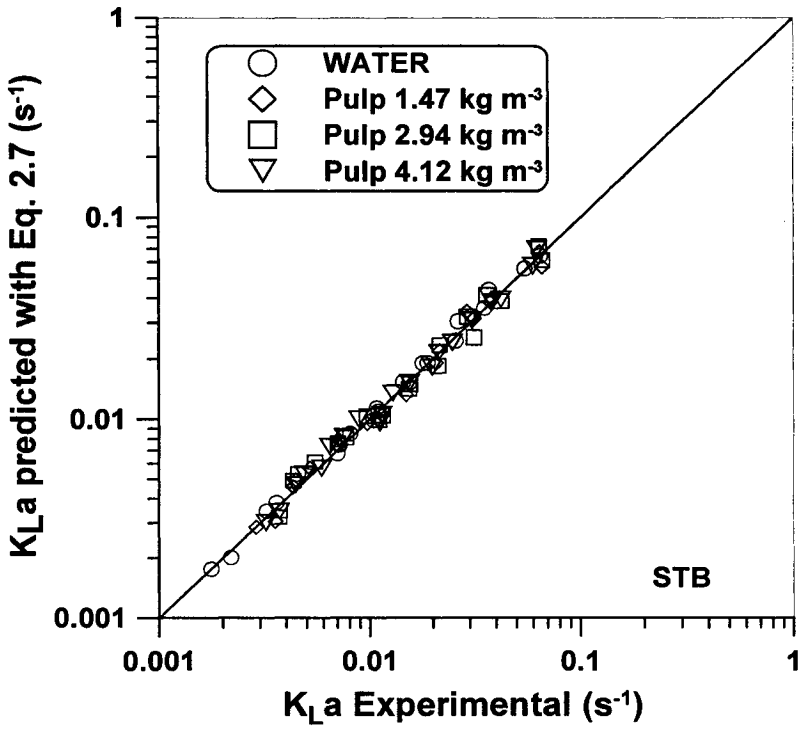

Figure 2.9 – Experimental versus calculated oxygen mass transfer coefficient for the STB.

Beyond this RPB threshold, the ratio steadily increases. In general, the K_La ratio reaches a minimum for intermediate power input per unit volume, located in the vicinity of the RPB power threshold. For low aeration flow rates, the ratio is generally lower than one, which suggests that the STB makes better use of its energy for small gas holdup. However, at higher aeration rates, the K_La ratio is nearly always above one and higher K_La is achieved in the RPB for an equal amount of power input per unit volume. This improved performance is due to a greater gas holdup and to lower power requirement with the RPB when the gas flow rate is increased. Lounes (1994) has shown that an increase in the gas holdup, resulting from an increase in gas flow rate, for the same speed of agitation led to a significant decrease in power necessary to reciprocate the plate stack.

It will be interesting to see the effect of the shear stress during the fermentation run with *Aspergillus niger* since, in many fermentations where shear sensitive microorganisms and products are involved, it is mandatory to operate the system at lower power per unit volume that is, corresponding to the first regime of operation or to the first portion of the second regime. The selection of the mixing intensity is a compromise between high oxygen mass transfer and low shear stress. The contribution of gas flow rate through the column will play an important role. In such a case, the mixing device will provide the necessary homogenization of the broth more than acting as a direct oxygenation promoter. Reciprocating plate columns therefore appear to be better suited for this application because of the relatively uniform mixing throughout the column. Selecting adequate mixing intensity is not a trivial task as it affects both biomass production and product formation. In addition, the mixing intensity profile may have to be adjusted in order to optimize production yield.

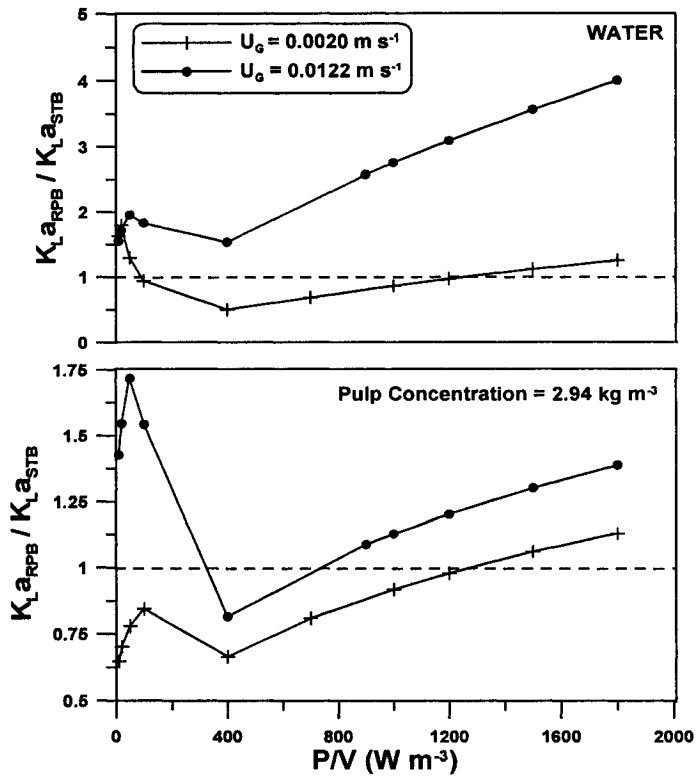

Figure 2.10 – Ratio of K_La obtained for the RPB and STB as a function of the power per unit volume for water and a solution with a pulp concentration of 2.94 kg/m^3.

2.5 Conclusion

A water-pulp fluid model was considered for characterizing the rheological properties of a fermentation broth of *Aspergillus niger*. Experimental data for power consumption and oxygen mass transfer in reciprocating plate and stirred tank bioreactors were presented. Plots of the oxygen mass transfer coefficient against power input per unit volume clearly showed two separate regimes for both bioreactors. In the first regime, the influence of power input per unit volume was not significant and K_La was mainly a function of the gas superficial velocity. However, above a certain threshold of power input per unit volume, K_La increases rapidly with an increase in the intensity of agitation. The oxygen mass transfer coefficient

was found to decrease with increasing pulp concentration in the RPB but it was found to be relatively constant in the STB.

The reciprocating plate bioreactor showed slightly favorable oxygen mass transfer especially for higher gas flow rates at a given power input per unit volume compared to the stirred tank bioreactor. This may be due to the fact that the reciprocating plate bioreactor provides more homogeneous mixing than the stirred tank bioreactor and less power is required at higher gas flow rates. Due to characteristics of the reciprocating plate bioreactor, it can be used for highly viscous, non-Newtonian broths and shear sensitive biological systems where it would be necessary to operate at lower agitation speeds and distribute more uniformly the power imparted to the fluid.

2.6. Nomenclature

A_c cross-sectional area of the column (m^2)

C unit conversion factor (dimensionless)

C_F dissolved oxygen concentration in liquid film ($kmolm^3$)

C_G dissolved oxygen concentration in gassed phase ($kmol/m^3$)

C_L dissolved oxygen concentration ($kmol/m^3$)

C_L^* saturated dissolved oxygen concentration in the solution ($kmol/m^3$)

C_P dissolved oxygen concentration recorded by the oxygen probe ($kmol/m^3$)

K_La overall oxygen mass transfer coefficient (s^{-1})

M torque required to rotate the system in the liquid (N m)

M_0 torque required to rotate the system in the air (N m)

N agitation speed (s^{-1})

P_G instantaneous pressure drop (kPa)

$\overline{P_G}$ average power input (W)

Δ_P instantaneous pressure drop (kPa)

t time (s)

T period of oscillation (s)

U_G gas superficial velocity (m s^{-1})

V_L liquid volume (m^3)

V_P instantaneous plate velocity (m s^{-1})

Z axial co-ordinate (m)

Greek letters

α parameter in Equation (7) (–)

β parameter in Equation (7) (–)

ε gas hold up (–)

γ parameter in Equation (7) (–)

τ_P time constant for oxygen probe (s)

2.7 References

Allen, D. G. and C. W. Robinson, "Hydrodynamics and Mass transfer in *Aspergillus niger* Fermentation in Bubble Column and Loop Bioreactors", Biotechnol. Bioeng., 34, 731-740 (1989).

Allen, D. G. and C. W. Robinson, "Measurement of Rheological Properties of Filamentous Fermentation Broths", Chem. Eng. Sci. 45, 37-48 (1990).

Audet, J., H. Gagnon, M. Lounes and J. Thibault, "Polysaccharide Production: Experimental Comparison of the Performance of Four Mixing Devices", Bioprocess Eng. 19, 45-52 (1998).

Audet, J., J. Thibault and A. LeDuy, "Polysaccharide Concentration and Molecular Weight Effects on the Oxygen Mass Transfer in a Reciprocating Plate Bioreactor", Biotechnol. Bioeng. 52, 507-517 (1996).

Baird, M. H. I. and N. V. Rama Rao, "Characteristics of Countercurrent Reciprocating Plate Bubble Column. II Axial Mixing and Mass Transfer", Can. J. Chem. Eng. 66, 222-231 (1986).

Bailey, J. E. and D. F. Ollis, "Biochemical Engineering Fundamentals", McGraw Hill, 2nd ed. (1986).

Gagnon, H., M. Lounes and J. Thibault, "Power Consumption and Mass Transfer in Agitated Gas-Liquid Columns: A Comparative Study", Can. J. Chem. Eng. 76, 379-389 (1998).

Jolicoeur, M., C. Chavarie, P. J. Carreau and J. Archambault, "Development of a Helical Ribbon Bioreactor for High-Density Plant Cell Suspension Culture", Biotechnol. Bioeng. 39, 511-521 (1992).

Linek, V., V. Vacek and P. Benes, "A Critical Review and Experimental Verification of the Correct Use of the Dynamic Method for the Determination of Oxygen Transfer in Aerated Agitated Vessels to Water", Chem. Eng. J. 34, 11-34 (1987).

Lounes, M., "Conception et performance de bioréacteurs à plateaux à mouvements alternatifs", Ph.D. Thesis, Laval University, Quebec, Canada (1994).

Lounes, M. and J. Thibault, "Hydrodynamics and Power Consumption of a Reciprocating Plate Gas-Liquid Column", Can. J. Chem. Eng. 71, 497-506 (1993).

Lounes, M. and J. Thibault, "Mass Transfer in a Reciprocating Plate Bioreactor" Bioprocess Eng. 13, 169-189 (1994).

Lounes, M., J. Audet, J. Thibault and A. LeDuy, "Description and Evaluation of Reciprocating Plate Bioreactors", Bioprocess Eng. 13, 1-11 (1995).

Nishikawa, M., M. Nakamura, H. Yagi and K. Hashimoto, "Gas Absorption in Aerated Mixing Vessel", J. Chem. Eng. Japan 14, 219-226 (1981).

Perez, J.F. and O. C. Sandall, "Gas absorption by Non-Newtonian Fluids in Agitated Vessels", AIChE J. 20, 770-775 (1974).

Popovic, M. K. and C. W. Robinson, "Mass Transfer Studies of External-Loop Airlifts and a Bubble Column", AIChE J. 35, 393-405 (1989).

Tecante, A. and L. Choplin, "Gas-Liquid Mass Transfer in Non-Newtonian Fluids in a Tank Stirred with a Helical Ribbon Screw Impeller", Can. J. Chem. Eng. 71, 859-865 (1993).

Thibault, J. and A. LeDuy, "Pullulan, Microbial Production Methods". In M.C. Flickinger and S.W. Drew, Encyclopedia of Bioprocess Biotechnology: Fermentation, Biocatalysis, and Bioseparation. John Wiley & Sons, Inc., 2232-2247 (1999).

CHAPTER 3

EVALUATION OF THE OXYGEN MASS TRANSFER IN *Aspergillus niger* FERMENTATION USING DATA RECONCILIATION

Nilesh Patel *and* Jules Thibault
Department of Chemical Engineering
University of Ottawa
Ottawa (ON), K1N 6N5, Canada

Abstract

Fermentation experiments done with *Aspergillus niger* results in a very viscous broth due to the growth of this filamentous microorganism. For this type of viscous fermentation process, it is difficult to estimate with confidence the oxygen mass transfer coefficient (K_La), which can be used for scale up or design of bioreactors. In the present study, four methods based on dynamic and stationary approaches were available to measure K_La during the fermentation process. Data reconciliation was used to obtain a more reliable and consistent K_La. The K_La value obtained by data reconciliation technique was found to be more reliable since it takes into consideration both the reliability of all measured variables and the accuracy of all mass balance equations.

Keywords: bioreactor, data reconciliation, fermentation, oxygen mass transfer coefficient.

3.1 Introduction

In aerobic fermentations, the availability of oxygen to the microorganism is critical for their growth and, subsequently, to the product formation. Many researchers have studied different types of bioreactors and mixing devices in an attempt to enhance the oxygen mass transfer to the fermentation mixture. The oxygen mass transfer coefficient (K_La) is an important scale up factor in designing bioreactors (Moo-Young and Blanch, 1981), and the most common parameter for evaluating the efficiency of oxygenation of a given type of equipment.

During submerged fermentation, K_La can be calculated using more than one method. The different methods can be broadly classified as dynamic and steady-state methods. Dynamic method consists of measuring the change in dissolved oxygen in the bioreactor during a step change in the inlet gas oxygen concentration. A prerequisite for using the dynamic method is to have a fast response dissolved oxygen probe for measuring the dissolved oxygen in the liquid medium. The steady state methods are based on either global oxygen or carbon dioxide balance of the gas phase entering and exiting the bioreactor. Therefore, an accurate measuring device is required to measure the inlet and outlet oxygen and carbon dioxide concentrations. At any instant during the fermentation, all methods should give an identical value of K_La but this is rarely the case. The difference in the estimation of K_La is due to the reliability of measured variables but also because the mass balance models are not perfect representations of the conditions prevailing in the fermentation broth (Brown, 1991). This makes it difficult to interpret the value of K_La and to use it confidently for assessing and designing oxygen mass transfer equipments. To overcome this difficulty, data reconciliation techniques can be used to improve the reliability of measurements in order to obtain a more

accurate and consistent value of K_La. Data reconciliation has been used successfully for many industrial processes (Romagnoli and Sanchez, 2000; Hodouin et al., 1993; Makni et al., 1995). Data reconciliation mainly consists of solving the K_La estimation problem by taking into account both the reliability of all measured variables and the accuracy of all mass balance equations.

The evaluation of K_La during *Aspergillus niger* fermentation was used to investigate the efficiency of the data reconciliation algorithm for estimating K_La during viscous fermentation processes. Fermentations were performed with two different types of bioreactors: reciprocating plate bioreactor (RPB) and stirred tank bioreactor (STB). In the data reconciliation strategy, an estimate of K_La was determined by minimizing an objective function involving 12 measured process variables and 4 mass conservation models. This chapter presents a description and discussion of the data reconciliation technique and the results obtained for the determination of K_La during the course of a viscous fermentation.

3.2 Materials and methods

The two bioreactors, a reciprocating plate bioreactor and a stirred tank bioreactor with three Rushton turbines, were used throughout these experiments. These bioreactors, built in our laboratories, are identical except for the mixing mechanism. The experimental setup is similar to the one used by Gagnon et al. (1998). The two bioreactors have a total volume of 22.5 L and a working volume of 17-18 L. The bioreactors are made of stainless steel and have an inner diameter of 228 mm and a column height of 550 mm. The outer tube has an internal diameter of 236 mm that leaves an annular gap of 3.5 mm where water, at an appropriate temperature, is continuously circulated to maintain the temperature of the

fermentation broth constant at 30 °C. The top of the bioreactor has ports for sampling and to hold a 19 mm dissolved oxygen probe (Ingold, Model 322756202) and a thermocouple. Compressed air or nitrogen from a cylinder is fed at the bottom of the bioreactor after passing through a rotameter, a mass flow meter (Matheson, Model 8273-0434) and a sterile gas filter. The gas sparger at the bottom of the bioreactor contains one hundred uniformly distributed holes, 1 mm in diameter. The gas flow rate is controlled by a mass flow meter and a dissolved oxygen probe measures the dissolved oxygen at a point located 82 mm from the centre of the column and 255 mm from the bottom of the reactor. The composition of the exit and inlet gas streams was measured with a Maihak, Multor 610. The O_2 was detected by paramagnetism while CO_2 was detected by infrared. The gas stream was dehumidified before analysis.

3.2.1 RECIPROCATING PLATE BIOREACTOR (RPB)

A schematic view of the plate stack used in the RPB is shown in Fig. 2.1. The plate stack consisted of 6 perforated stainless steel plates, 221 mm in diameter and 1.25 mm thick. Each plate was spaced 50 mm apart from one another. The perforations have a diameter of 19 mm and holes are distributed on an equilateral triangular pitch. The plate fractional free area, including the 3.5 mm annular space between the plate edge and bioreactor wall, is 0.357. The power imparted by the plate stack to fermentation medium is calculated from variations in the pressure at the base of the column. Instantaneous pressure is measured by a pressure transducer (Ashcroft, Stratford, Connecticut Model H-68845-52) connected to the bottom of the bioreactor. The power input was calculated using the method proposed by Lounes and Thibault (1993). The driving unit consists of a connecting rod, which imparts the

reciprocating motion, a tenfold reducing speed transmission and a variable speed motor controlled by a microcomputer. An aluminum disc, containing 100 uniformly distributed perforations and mounted on the output shaft of the reducing transmission, is used in conjunction with an infrared optical switch (HOA-2001, Honeywell) to measure and control, with a microcomputer, the frequency of the reciprocation by manipulating the power to the motor.

3.2.2 STIRRED TANK BIOREACTOR (STB)

A schematic view of the mixing device used in the stirred tank bioreactor is shown in Fig. 2.2. The three identical Rushton turbines were mounted on the central shaft. The location of the impellers, measured from the bottom of the column, is 56, 199 and 327 mm. Each turbine has 6 blades mounted on the periphery of a 50 mm diameter disk. Each blade is 25 mm long, 15 mm high and 1.5 mm thick. Four baffles, 375 mm high, 16 mm wide and 1 mm thick, were placed inside the mixing vessel.

The impeller shaft is driven by a mechanical system composed of a motor (90 VDC, 1800 RPM, ½ HP, Frame 56C, Model 8293, Pacific-Scientific) and a ten-to-one speed reducer assembly (Model 201657, Doerr Electric). A speed controller (Multi-Drive Model KBMD-240D, KB Electronics, Inc.) connected to the motor allows a variable speed in both clockwise and counter-clockwise rotation. Torque is measured with a non-contact strain gage torquemeter (S. Himmelstein & Co., Model MCRT 25-02T, 25-0). The operating range for the torque and the speed are 0 to ±2.82 Nm and 0 to 1000 RPM, respectively. The torque and speed output signals were amplified and read on the digital display of a modular unit (S. Himmelstein & Co. System 6 recorder including a digital counter Model 6-206b, a

transducer amplifier model 6-201 and scanner Model 6-405B). The recorder has an analog voltage output that allows the torque and speed to be read by a microcomputer. For the stirred tank bioreactor, the power input was calculated using torque and rotational speed.

3.2.3 EXPERIMENTAL PROCEDURE

The microorganism used for the fermentation experiment was *Aspergillus niger* obtained from American Type Culture Collection (ATCC 1015). The freeze-dried culture was rehydrated and grown on Petri dish and subsequently transferred to an agar slant. It was then used to inoculate a 50 ml of culture medium. The composition of the culture medium (Atkinson and Mavituna, 1991) was identical for both bioreactors and given in Table 3.1. Three days before the start of experiment, the microorganisms were transferred into two 730-ml Erlenmeyers of culture medium. The bioreactors and its contents were autoclaved for a period of 20 min at 121 ^{o}C and 0.2 MPa (15 psig). At the start of each experiment, one Erlenmeyer was transferred into each bioreactor containing about 17 L of culture solution. The RPB was run at frequencies of 0.25, 0.5, 0.75, and 1.00 Hz with superficial gas velocities of 0.0041 m/s (0.6 VVM). The STB was run at 100, 200, 300 and 400 RPM with identical gas flow rate as the RPB. A sample was collected daily from each bioreactor and was analyzed for biomass, pH, citric acid and sugars. Samples were first centrifuged at 15 000 RPM for 20 minutes and then the supernatant was filtered using a pre-weighted 45 μm Gelman filter (Gelman Sciences Inc glass fiber filter, Type A/E, 47 mm, Prod. No. 61631). The biomass was resuspended in distilled water to leach out residual sugars and nutrients, and centrifuged again. The supernatant and biomass were filtered. The filter and the biomass

were placed in an oven (dryer) for 20 hours at 85-90 °C before measuring the dry weight of biomass. Each experiment was run for duration of 12-13 days.

Table 3.1 - Composition of the growth medium for *Aspergillus niger* fermentation

Components	**Concentration (kg/m^3)**
Sucrose	140
NH_4N0_3	2.5
KH_2PO_4	2.5
$MgSO_4 \cdot 7H_2O$	0.25

3.3 Theoretical background

3.3.1 K_La MEASUREMENT

The overall oxygen mass transfer coefficient was determined using the dynamic method (Taguchi and Humphrey, 1966; Lounes and Thibault, 1993) and the overall gas balance method. When the dissolved oxygen in the bioreactor was high, it was possible to use both methods whereas for low dissolved oxygen concentration, it was only possible to use the gas balance method. These two methods are based on equation (3.1), which states that the rate of change of the dissolved oxygen concentration in the fermentation medium is equal to the rate of oxygen mass transfer from the gas to the liquid phase minus the rate of the oxygen utilization rate by the microorganisms.

$$\frac{dC_L}{dt} = K_L a\left(C_L^* - C_L\right) - Q_{O2}X \tag{3.1}$$

3.3.2 DYNAMIC METHOD

The dynamic method, first proposed by Taguchi and Humphrey (1966), is used to determine both the oxygen uptake rate and K_La at one instant during the fermentation. This method consists in stopping temporarily the gas flow into the bioreactor to eliminate the addition of oxygen to the liquid broth such that the decrease in dissolved oxygen concentration in the bioreactor can be attributed entirely due to its consumption by the microorganism. At the same time, the speed of agitation is completely stopped or reduced to its minimum to prevent cells settling at the bottom of the bioreactor (Gagnon et al., 1998). The slope obtained by plotting C_L versus time, which usually is a straight line, provides an estimate of the oxygen uptake rate ($Q_{O_2}X$). Before the dissolved oxygen reaches its critical value, the air is reintroduced into the bioreactor and agitation resumed. A typical plot of the experimental dissolved oxygen concentration as a function of time during the dynamic method is presented in Fig. 3.1.

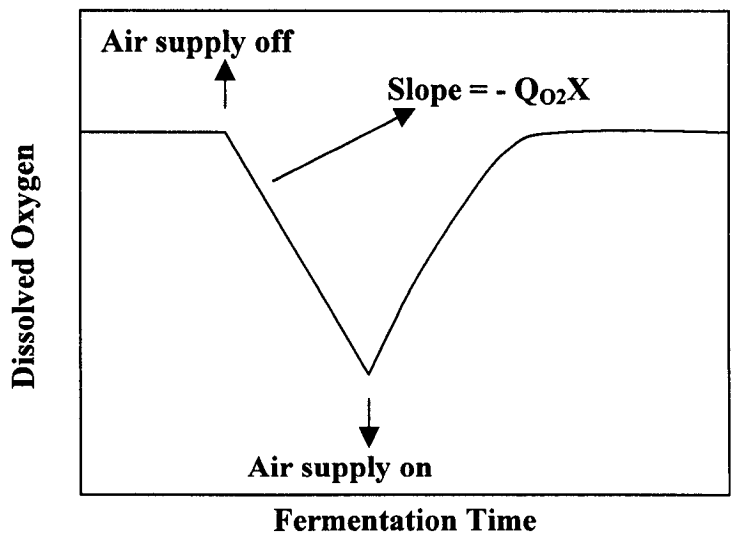

Figure 3.1 – Determination of the oxygen mass transfer coefficient using the dynamic method.

Having an estimate of the oxygen uptake rate, the value of K_La can be determined from the rate of change of the dissolved oxygen up to its stationary value. K_La can be calculated by rearranging equation (3.1).

$$C_L = C_L^* - \frac{1}{K_L a}\left(\frac{dC_L}{dt} + Q_{O2}X\right) \tag{3.2}$$

K_La can be easily obtained graphically from the slope of equation (3.2) or calculated by solving numerically equation (3.1). A numerical solution has the advantage to allow easily incorporating the dynamics of the dissolved oxygen probe. Appreciable errors, especially for higher values of K_La, may result if the probe dynamics is neglected. It is worth noting that the estimation of K_La does not depend upon the quality of the estimation of the value of $Q_{O_2}X$, obtained in the first step (Dorresteijn et al., 1994).

3.3.3 STATIONARY METHODS

With the availability of more accurate gas analyzer or mass spectrometer, K_La can be calculated using three additional methods using the information obtained under stationary conditions. Under pseudo-steady-state conditions, Equation (3.1) can be rearranged to calculate K_La as follows:

$$K_L a = \frac{Q_{O2}X}{C_L^* - C_L^0} \tag{3.3}$$

This equation requires an estimate of $Q_{O_2}X$ that can be easily obtained from the dynamic method as previously explained. This method is referred to as the stationary method. An estimate of $Q_{O_2}X$ can also be obtained using the difference in oxygen concentration between the inlet and exit gas streams since it represents the oxygen consumption by microorganisms. Therefore, this oxygen uptake rate can be used to calculate the K_La using the equation (3.4).

$$K_L a = \frac{\frac{1}{V_L}\left(\frac{P_1}{R T_1} Q_{1,G}\, y_{1,O2} - \frac{P_2}{R T_2} Q_{2,G}\, y_{2,O2}\right)}{(C_L^* - C_L^o)} \tag{3.4}$$

Similarly, if the respiratory quotient (RQ) is known, the carbon dioxide production rate can be used to calculate $K_L a$ using equation (3.5).

$$K_L a = \frac{\frac{1}{RQ}\frac{1}{V_L}\left(\frac{P_2}{R T_2} Q_{2,G}\, y_{2,CO2} - \frac{P_1}{R T_1} Q_{1,G}\, y_{1,CO2}\right)}{(C_L^* - C_L^o)} \tag{3.5}$$

Usually, RQ is available for most of the common fermentation processes. Otherwise, it can easily be estimated from past fermentation experiments.

All these four methods have their own strengths and limitations at different stages of the fermentation process. For example, the dynamic method can be used with relatively higher precision during the initial stages of fermentation as the oxygen consumption is low and the dissolved oxygen concentration in the medium is high. Because of the low oxygen consumption, the difference between the inlet and exit gas concentrations is consequently very small at that stage of fermentation, and the gas balance methods for $K_L a$ estimation lack accuracy. As the fermentation progresses, the growth of biomass leads to an increase in oxygen consumption and to a decrease in the concentration of dissolved oxygen. As a result, the gas balance methods provide more accurate $K_L a$ estimations. However, at one point, the dissolved oxygen concentration may become too low to allow using the dynamic method and one has to rely strictly on the gas balance methods. Fortunately, it is under these circumstances that the gas balance methods provide the most accurate estimates of the values of $K_L a$. Because the relative accuracy of the various methods constantly varies throughout the fermentation, averaging the values of $K_L a$ will not lead to the best estimate. To overcome this problem and to take into account the relative accuracy of all methods, a data

reconciliation technique was used. This technique, in addition to consider the precision of each method, takes into account the reliability of all measurements involved in the estimation of K_La values.

3.3.4 DATA RECONCILIATION TECHNIQUE

There is some degree of error associated with any variable measured during the fermentation process. This error should be removed or minimized before using these values for process analysis, optimization and control. The technique of data reconciliation was the subject of numerous research works (Crowe, 1989; Mah, 1990; Liebman et al., 1992). Data reconciliation appears to be well suited for the present K_La estimation problem since we have a series of process measurements along with dynamic and stationary oxygen conservation equations that should lead to a single K_La value. Pouliot et al. (2000) have used this technique to reconcile the data and estimate K_La for a fermentation process involving the production *Saccharomyces cerevisiae* (Baker's yeast). In the case of *S. cerevisiae*, the oxygen utilization rate is much higher than the one for the microorganism *Aspergillus niger* used in the present investigation, and the difference in oxygen and CO_2 concentrations was significantly higher throughout the fermentation.

Akin to the errors affecting measured variables, oxygen conservation models are prone to model mismatch since they are rarely perfect representations of the fate of the oxygen in a fermentation process. Therefore, data reconciliation may be used to obtain a better estimate of K_La whereby the level of confidence that one has in both the measured variables and the oxygen conservation models are taken into account.

To calculate K_La during the fermentation process a number of measured and estimated values are required. In the current set of experiments, 12 measured or estimated variables

were required to evaluate the oxygen mass conservation models. These variables are: the pressure (P), the temperature (T), the time constant of the dissolved oxygen probe (τ_P), the saturation dissolved oxygen concentration (C_L^*), the dissolved oxygen concentration (C_L), the liquid volume (V_L), the respiratory quotient (RQ), the gas flow rate (Q_G), the oxygen mole fraction in the inlet ($y_{1,O2}$) and exit ($y_{2,O2}$) gas streams, and the carbon dioxide mole fraction in the inlet ($y_{1,CO2}$) and exit ($y_{2,CO2}$) gas streams. An objective cost function, consisting of the weighted sum of all 12 measured or estimated variables, and six oxygen mass conservation models, can be defined and solved to determine the best estimate of the value of K_La. To better understand how this objective function is constructed, it was divided into partial objective functions. The first partial objective function contains all measured/estimated and adjusted values of the twelve process variables, and it is represented as follows:

$$J_1 = \alpha_1\left(\hat{P}-P\right)^2+\alpha_2\left(\hat{T}-T\right)^2+\alpha_3\left(\hat{\tau}_P-\tau_P\right)^2+\alpha_4\left(\hat{\tilde{C}}_L^*-\tilde{C}_L^*\right)^2+\alpha_5\left(\hat{C}_L^0-C_L^0\right)^2+$$
$$\alpha_6\left(\hat{V}_L-V_L\right)^2+\alpha_7\left(\hat{RQ}-RQ\right)^2+\alpha_8\left(\hat{Q}_G-Q_G\right)^2+\alpha_9\left(\hat{y}_{1,O2}-y_{1,O2}\right)^2+ \quad (3.6)$$
$$\alpha_{10}\left(\hat{y}_{2,O2}-y_{2,O2}\right)^2+\alpha_{11}\left(\hat{y}_{1,CO2}-y_{1,CO2}\right)^2+\alpha_{12}\left(\hat{y}_{2,CO2}-y_{2,CO2}\right)^2$$

Each term of this equation represents the difference between the measured/estimated and adjusted values of a process variable, the adjusted variable being represented with an overscript caret. In solving the overall objective function, the adjustment of each variable with respect to its measured/estimated value will depend on the weight factor α and their impact on the oxygen conservation models. The second partial objective function comes from the first portion of the dynamic method, and it is used to estimate the value of $Q_{O_2}X$

from the slope of the decrease in the dissolved oxygen concentration when the aeration is stopped.

$$J_2 = \alpha_{13}\left(\frac{dC_L}{dt} + \hat{Q}_{O2}X\right)^2 \tag{3.7}$$

The second portion of the curve in the dynamic method, which provides an estimation of K_La, is represented by the third partial objective function.

$$J_3 = \alpha_{14}\left(C_L - \left(\hat{C}_L^* - \frac{1}{\hat{K}_L a}\left[\frac{dC_L}{dt} + \hat{Q}_{O2}X\right]\right)\right)^2 \tag{3.8}$$

As explained earlier, K_La can be determined by evaluating the slope of the curves obtained in the dynamic method. While solving the second and third partial objective functions, the dynamics of the dissolved oxygen probe was also taken into consideration by using the first-order differential equation:

$$\hat{\tau}_P \frac{d\hat{C}_P}{dt} = \hat{C}_L - \hat{C}_P \tag{3.9}$$

The partial objective functions J_2 and J_3 were therefore set equal, for the two portions of the dynamic response curve, to the average difference between the predicted and experimental dissolved oxygen concentration, as measured by the probe. The dynamic response of the measured dissolved oxygen concentration for both portions of the dynamic method was simulated by finite differences using the most current adjusted values of the variables.

The partial objective function (J_4) estimates K_La using the stationary method represented by equation (3.3).

$$J_4 = \alpha_{15}\left(\hat{K}_L a - \frac{\hat{Q}_{O2}X}{\hat{C}_L^* - \hat{C}_L^0}\right)^2 \tag{3.10}$$

Similarly, the partial objective functions J_5 and J_6 use the overall O_2 and CO_2 gas balance methods to estimate K_La.

$$J_5 = \alpha_{16}\left(\hat{K_L a} - \frac{1}{\hat{C}_L^* - \hat{C}_L^0}\frac{1}{\hat{V}_L}\frac{\hat{P}}{R\hat{T}}\hat{Q}_G\left(\hat{y}_{1,O2} - \hat{y}_{2,O2}\right)\right)^2 \tag{3.11}$$

$$J_6 = \alpha_{17}\left(\hat{K_L a} - \frac{1}{\hat{C}_L^* - \hat{C}_L^0}\frac{1}{\hat{V}_L}\frac{1}{\hat{RQ}}\frac{\hat{P}}{R\hat{T}}\hat{Q}_G\left(\hat{y}_{2,CO2} - \hat{y}_{1,CO2}\right)\right)^2 \tag{3.12}$$

It is reasonable to assume an identical gas flow rate, pressure and temperature for the outlet and inlet gas streams since the gas streams are dehumidified before being analyzed and the respiratory quotient (RQ) is close to unity.

An additional partial objective function (J_7) was included into the overall objective function to take into account the effect of the average gaseous oxygen concentration within the fermenter, the total pressure and the chemical components of the fermentation broth.

$$J_7 = \alpha_{18}\left(\hat{C}_L^* - \hat{\tilde{C}}_L^*(\hat{T},S)\frac{\hat{y}_{1,O2} + \hat{y}_{2,O2}}{2\,\tilde{y}_{O2}}\frac{\hat{P}}{\tilde{P}}\right)^2 \tag{3.13}$$

The value of the saturation dissolved oxygen concentration (C_L^*) was evaluated at the temperature of the fermenter broth and corrected for its initial chemical composition (Schumpe et al., 1978). Thus the overall objective function is the summation of the seven partial objective functions:

$$J = J_1 + \beta\left(J_2 + J_3 + J_4 + J_5 + J_6 + J_7\right) \tag{3.14}$$

The parameter β is an additional weighting factor that is used to put more or less emphasis on the oxygen conservation models with respect to the measurements. It is normally equal to one.

Weighting Factors and Monte Carlo Technique

As discussed earlier, to solve the objective function, weighting factors (α_i, $i \in (1,18)$) must be specified. These weighting factors depend on the level of confidence on each measured/estimated process variable and each oxygen conservation model. Assuming that measurement errors are normally distributed, the level of confidence of a process variable is related to its variance. The weighting factor for each measurement term was therefore set equal to its inverse variance. The estimation of the variance of each measurement considers the accuracy of the sensing device, calibration errors, stability of the signal over a period of time, and measurement errors. Table 3.2 gives the estimated precision ($\pm 3\sigma$) of each process variable that is required by the oxygen conservation models to determine $K_L a$. Table 3.2 also gives the corrected value after reconciliation of each process variable for a typical fermentation performed in this investigation. The time constant of the dissolved oxygen probe (τ_P) was evaluated with separate experiments in water under identical conditions of agitation and aeration.

The estimation of $K_L a$ values using the oxygen conservation models largely depends on the precision of measurements used in each conservation model. Weighting factors of conservation models must therefore be determined considering the individual precision of each measured variable. Since the precision of each conservation model varies during the course of the fermentation, it is necessary to determine the weighting factors for each individual experimental test performed at regular time intervals. For instance, in the last portion of the exponential growth phase, provided that all other operating conditions remain identical, the estimation of $K_L a$ using the oxygen and carbon dioxide mass balance is more accurate because the differences between the input and the output concentrations are larger.

Table 3.2 - Estimated values obtained for each process variable during a typical fermentation and estimated precision (± 3σ) of each variable.

Parameter	Measured	Reconciled	Precision (± 3σ)
P	101300 Pa	100100 Pa	3000
T	303.2 K	303.2 K	1
τ_P	17.0 s	16.84 s	2
$\tilde{C}_L^*$	0.2334 mol/m^3	0.2310 mol/m^3	0.00625
C_L	0.1781 mol/m^3	0.1403 mol/m^3	0.00625
V_L	0.01653 m^3	0.01653 m^3	0.0001
RQ	1.0	0.9945	0.2
Q_G	0.000167 m^3/sec	0.000167 m^3/sec	1.66 * 10^{-6}
$y_{1,O2}$	0.2095	0.2095	0.001
$y_{2,O2}$	0.2077	0.2073	0.002
$y_{1,CO2}$	0.00035	0.00035	0.0005
$y_{2,CO2}$	0.002700	0.002724	0.001

To obtain the respective weighting factors for each individual experiment, a Monte Carlo simulation method was used. Monte Carlo simulation is a mathematical technique for numerically solving differential or algebraic equations. It is used extensively in science to solve many problems for which no other solutions exist. It consists of using random numbers to generate a large number of possible scenarios and the results of the many scenarios are analyzed statistically to obtain information on estimated average value and variability of possible results. The answers are always approximate, but with sufficient number of scenarios, tend to converge to the theoretical answers. In the present investigation, 1000 simulations were performed to evaluate partial objective functions J_2 to J_7. In each simulation, the 12 process variables were generated in the range of ±3σ of each variable

measured at each fermentation time using random Gaussian numbers. Then, the variance of each partial objective function was evaluated in order to provide the relative accuracy of each oxygen conservation term in the overall objective function. The inverse of the calculated variance of each partial objective function was used as the weighting factor.

3.4 Results and discussion

3.4.1 OXYGEN MASS TRANSFER COEFFICIENT

Throughout the fermentation, the oxygen utilization rate initially increases as the concentration of biomass increases. At the beginning and at the end of the experiment, the dynamic method is more accurate than the gas balance methods because of the small difference between the inlet and exit gas concentrations. However, as the fermentation progresses and more biomass is being produced, the dissolved oxygen concentration in the medium decreases and the difference of O_2 and CO_2 concentrations between the input and output gas streams increases. For higher levels of agitation, the dissolved oxygen concentration in the medium normally remains sufficiently high to calculate the K_La using the dynamic method whereas for lower agitation levels, the dissolved oxygen may attain a critically low concentration making impossible using the dynamic method. Because of the low dissolved oxygen concentration, one has to rely only on the gas balance methods to calculate K_La. This does not mean that the estimated value of K_La is not accurate. At this point, the gas balance methods become more accurate and reliable because of the relatively higher difference between the inlet and outlet O_2 and CO_2 gaseous concentrations.

In the present investigation, the type of bioreactors and the degree of agitation used during the fermentation process had a significant impact on the amount of biomass produced and

subsequently on the amount of dissolved oxygen concentration in the fermentation medium. There was a steep increase in biomass production for experiments conducted in the RPB whereas the increase in biomass was more gradual for experiments conducted in the STB (Fig 3.2). The amount of biomass produced in the RPB lies between 20 kg/m^3 and 30 kg/m^3 whereas the range of concentration in the STB is between 5 and 20 kg/m^3. The amount of biomass produced for experiments conducted in the RPB at 1.0 Hz was very high and resulted in a mechanical failure of the bioreactor due to the force that had to be exerted for mixing the high-cell concentration broth. These results show that the RPB is a very efficient bioreactor for producing higher biomass concentration. However, the rate of production of citric acid in the RPB (results not shown) always remained very low. It has been demonstrated that the production of citric acid will be low if the dissolved oxygen concentration falls below a threshold value (Kubicek et al., 1980). If this threshold dissolved oxygen concentration is reached, the substrate will be preferably used to produce biomass.

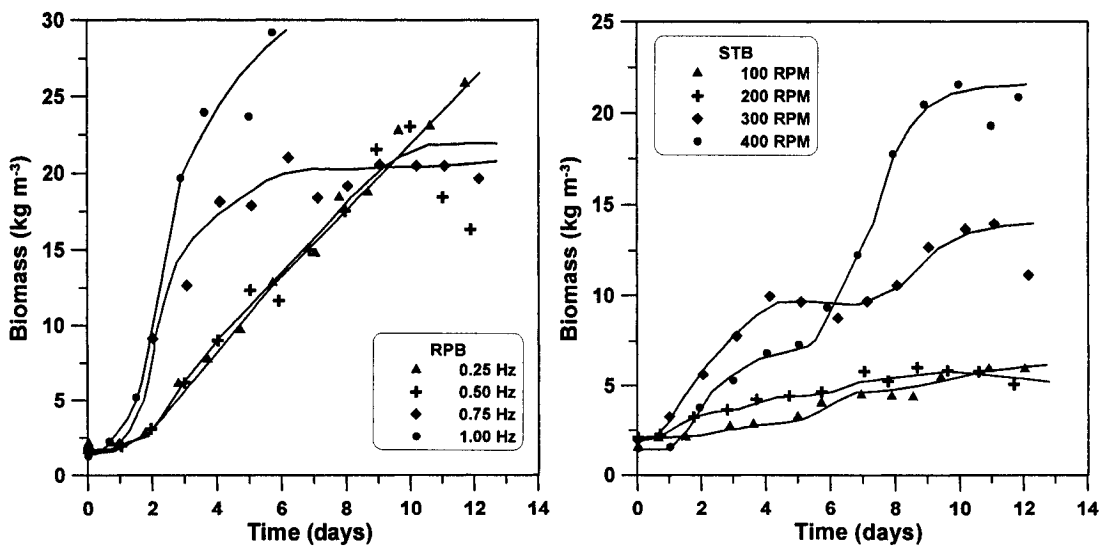

Figure 3.2 – Biomass concentration as a function of time for experiments conducted in the RPB and the STB at different agitation intensities.

Figure 3.3 presents the variation of the dissolved oxygen concentration over the twelve days of fermentation. In all experiments conducted in the RPB, the dissolved oxygen concentration decreases rapidly to a very low concentration and remains low for an extended period of time. On the other hand, the dissolved oxygen concentration in the STB always remained relatively high. The STB seems to be a preferred device for producing citric acid since it is generally accepted that the growth of production strain should be restricted for citric acid production (Röhr et al., 1983).

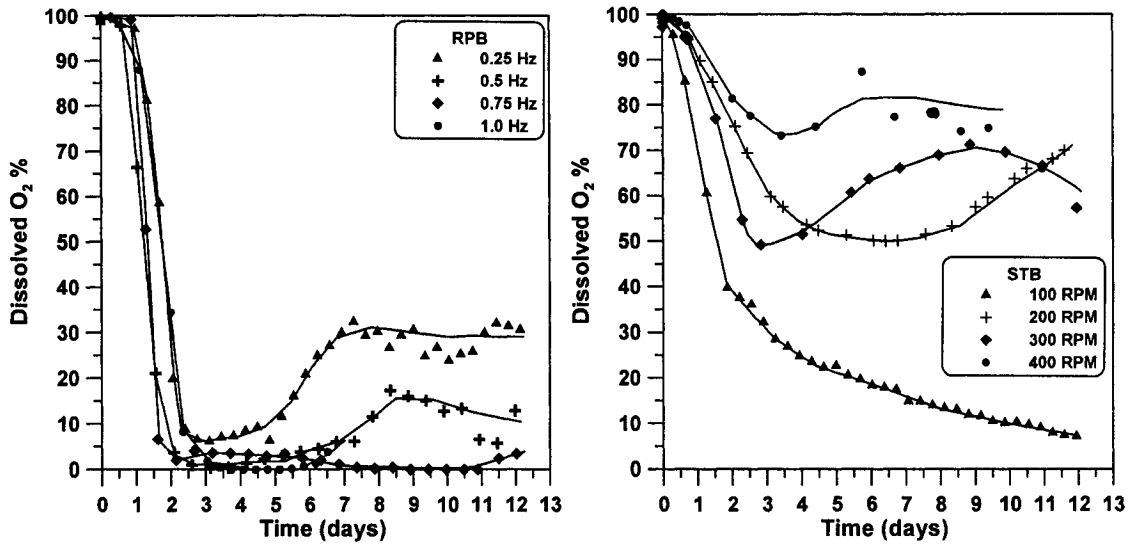

Figure 3.3 – Dissolved oxygen profiles for experiments conducted in the RPB and STB at different agitation intensities.

From a K_La estimation point of view, it is clear from the plot of Fig.3.3 that the dynamic method can only be used for the first few days of fermentation when conducted in the RPB whereas, for the STB, all the four methods were used to calculate K_La for the entire fermentation except when the agitation was 100 RPM. Typically the fermentation experiments were run between 12 to 13 days and the data reconciliation technique was used every 24 hours to estimate the value of K_La. When all four methods were available, 12 measured variables and 4 mass conservation models were used to calculate K_La using data

reconciliation. For each set of data, Monte Carlo simulations were performed to determine the respective weighting factors for partial objective functions J_2 to J_7. The overall objective function was minimized using a quasi-Newton optimization routine in order to obtain adjusted values of the 12 measurements of Table 3.2 as well as estimates of $Q_{O_2}X$ and K_La, for a total of 14 parameters. Initial estimates of $Q_{O_2}X$ and K_La were obtained using the method of Taguchi and Humphrey (1966) and, only for these initial estimates, the dynamics of the dissolved oxygen probe was not included. The time series of dissolved oxygen data generated during the dynamic method was split into its two segments associated with the two partial objective functions (J_2 and J_3) used to minimize the sum of squares of the difference between the experimental and predicted responses of the dissolved oxygen probe. Fig. 3.4 compares the predicted response, using the converged values of K_La and $Q_{O_2}X$, with the experimental data for the test conducted in the STB at 300 RPM on day 3.

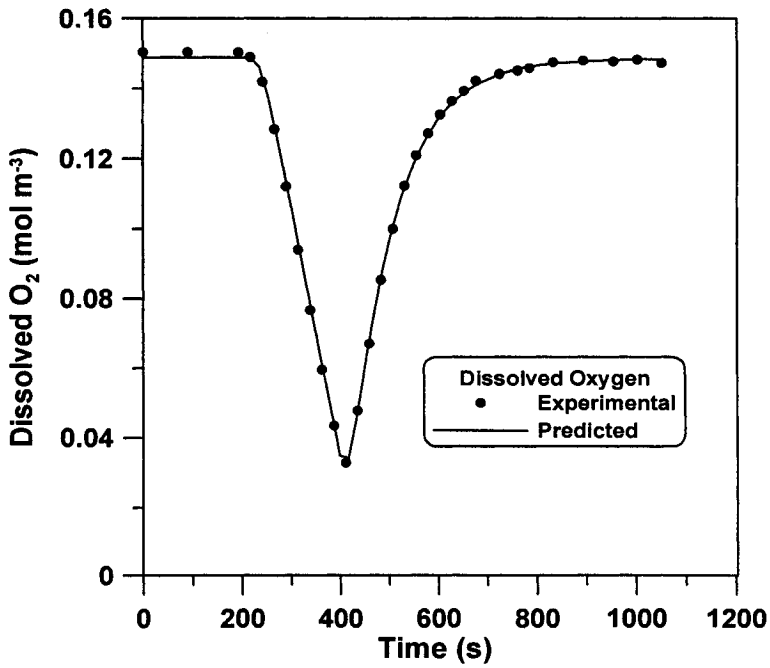

Figure 3.4 – Experimental and predicted dissolved oxygen concentrations during the dynamic method (STB at 300 RPB on day 3).

When the dissolved oxygen concentration was too low to allow using the dynamic method, it was only possible to use the gas balance methods to calculate the value of K_La. In this case, the same procedure was used except that the partial objective functions J_2 and J_3 were eliminated.

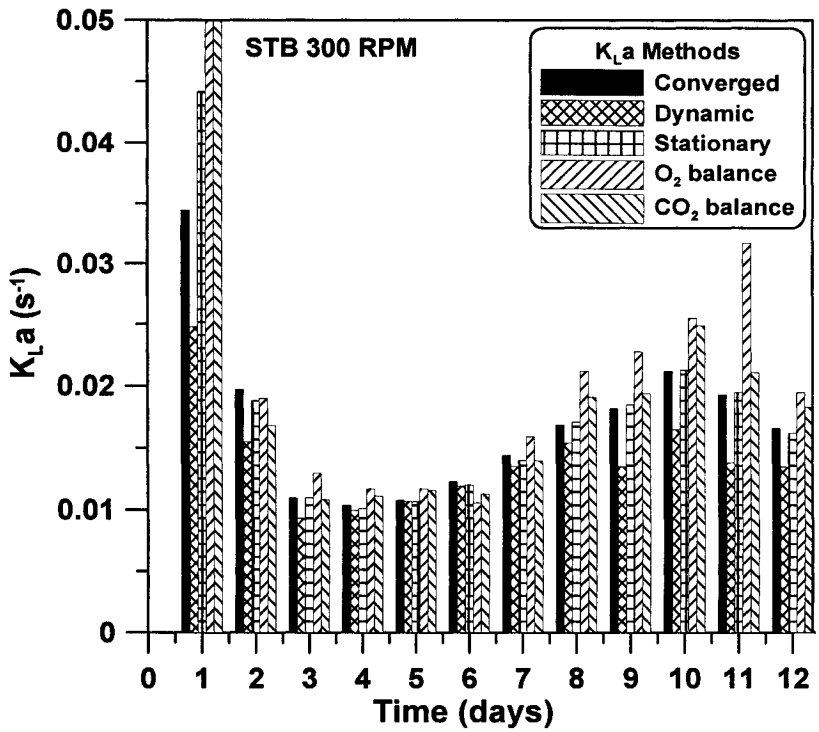

Figure 3.5 – K_La values obtained by four different methods and the final converged value as a function of time for the STB at 300 RPM.

Fig. 3.5 shows a plot of K_La data obtained daily for experiments conducted in the STB at 300 RPM. The dissolved oxygen concentration remained significantly high (Fig. 3.3) to calculate K_La by all four methods. At the beginning of fermentation, the estimation of K_La values obtained from the two gas balance methods are less reliable due to the lower differences between the inlet and exit O_2 and CO_2 gaseous concentrations. This lower precision is taken into consideration via lower weighting factors affecting partial objective functions J_5 and J_6. The converged value of K_La obtained by data reconciliation is closer to

the K_La value obtained with the dynamic and stationary methods. As can be observed in the Fig. 3.5, after few days of fermentation, the converged value of K_La becomes closer to the value obtained with the gas balance methods.

The profile of K_La as a function of time shows that K_La initially decreases then remains constant for a period of 4-5 days before increasing toward the end of fermentation. This pattern was observed for all experiments conducted in the STB. It is hypothesized that K_La decreases due to an increase in the viscosity of the fermentation broth associated with the growth of biomass. In addition, throughout the fermentation, the shearing action of the mixing device breaks some of the filamentous microorganisms and tends to reduce the viscosity of the broth. It is believed that the increase in K_La in the later stage of fermentation is associated with the termination of microorganism growth and the continued shearing of the long filaments of the microorganism.

The variation of K_La as a function of time for experiments conducted in the STB at 100 RPM are shown in Fig. 3.6 and for experiments conducted in the RPB at 0.75 Hz are shown in Fig. 3.7. As the fermentation progressed, the dissolved oxygen concentration for both experiments became too low (Fig 3.3) to use the dynamic method and thus the K_La had to be estimated using only the gas balance methods. The decrease in dissolved oxygen for the experiment conducted in the STB at 100 RPM was due to the relatively low agitation speed, whereas, the decrease in dissolved oxygen concentration in the RPB can be attributed to the high growth rate of microorganism and lower K_La values. However, for both cases, the data reconciliation technique was used successfully to calculate a good estimate of K_La.

There was a decrease in K_La followed by an increase for the fermentation performed in the STB at 100 RPM similar to the pattern observed in the STB at 300 RPM (Figure 3.5) whereas, the K_La value remained nearly constant for experiments performed in the RPB. This

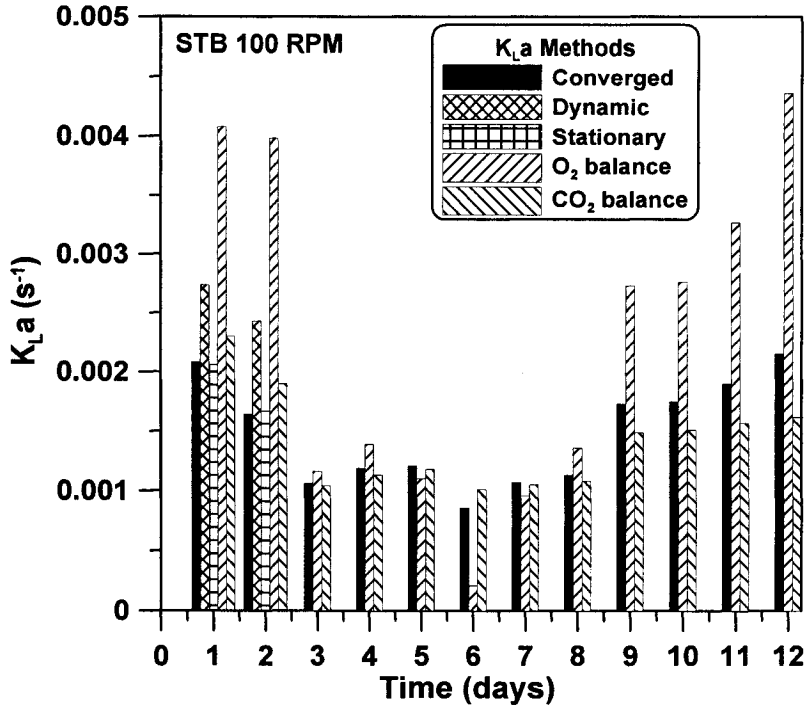

Figure 3.6 – K_La values obtained by four different methods and the final converged value as a function of time for the STB at 100 RPM.

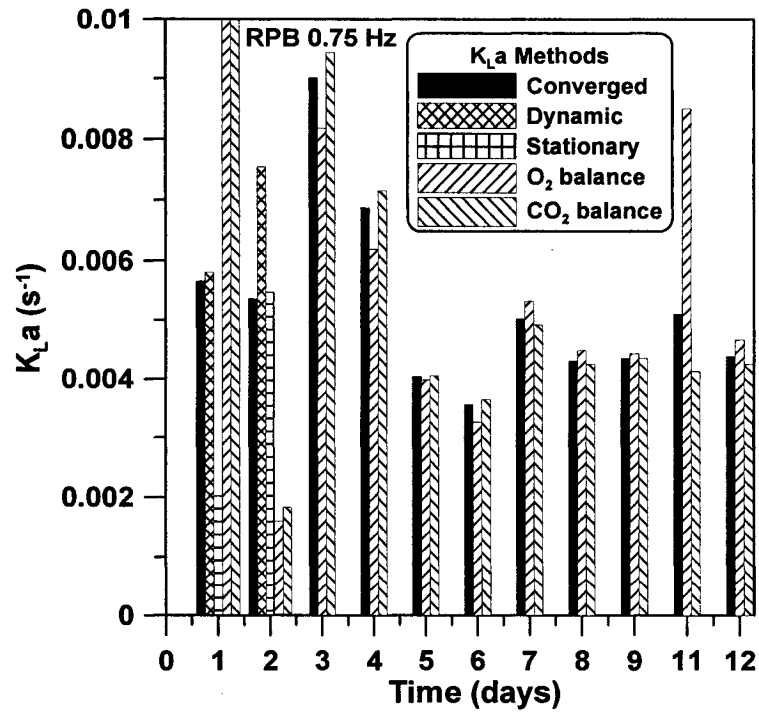

Figure 3.7 – K_La values obtained by four different methods and the final converged value as a function of time for the RPB at 0.75 Hz.

different behavior observed between the STB and RPB can be seen on the plot between the converged K_La obtained by data reconciliation technique and the biomass produced for the three experiments discussed previously (Fig. 3.8).

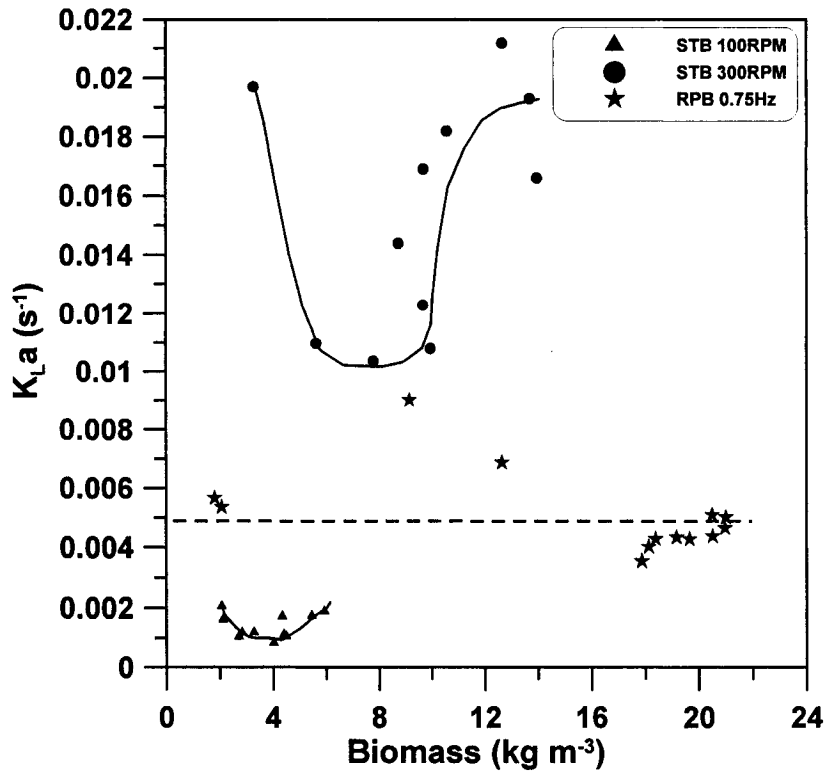

Figure 3.8 – Plot of K_La values obtained for fermentations conducted in the RPB and the STB versus biomass produced.

In data reconciliation, all measured/estimated variables are slightly modified to satisfy the model mismatch. If the level of uncertainty of one variable is high, then this particular variable could be corrected more than another variable having a higher degree of confidence. For example, the gas flow rate was measured very accurately and the weighting factor affecting the corresponding term in the objective function J_1 is very high, which precludes the new estimate of the flow rate to deviate significantly from its measured value. On the other hand, the estimate of RQ contains a higher uncertainty and it can vary during the

fermentation process. Therefore, the data reconciliation technique can modify the RQ value more significantly to better satisfy the mass balance models.

To evaluate the reliability of the data reconciliation algorithm for the estimation of K_La, a sensitivity analysis was performed. Using the nominal values of P, T, τ_P, $\tilde{C}_L^*$, V_L, RQ, Q_G, $y_{1,O2}$, and $y_{1,CO2}$, and set values of K_La and $Q_{O_2}X$, the four oxygen conservation models were used to simulate typical fermentation data: (1) dissolved oxygen profile for both the stationary phase before a dynamic test is performed, and during the dynamic method, and (2) the exit O_2 and CO_2 gaseous concentration. Each of the twelve variables of Table 3.2 was randomly corrupted by Gaussian noise using their estimated standard deviation. Then, the weighting factors for each model were calculated using the Monte Carlo procedure described above. This compete set of simulated data represents a typical fermentation, and each set of data was used to estimate K_La with all individual methods and with the data reconciliation algorithm. This procedure was repeated 1000 times to determine the average value of the estimated K_La and the standard deviation associated with each method.

All estimation methods gave an average value of K_La that was essentially equal to the set K_La value. One exception is the stand-alone dynamic method, which gave a slightly higher K_La average because the probe dynamics was not included for its determination. However, as mentioned above, the dynamics of the dissolved oxygen probe was included when the dynamic method was considered in the data reconciliation algorithm. The normalized standard deviation for the estimated K_La for each method varied significantly. Figure 3.9 presents a plot of the normalized standard deviation of each method and the converged value as a function of the ratio of the oxygen utilization rate and the real K_La value. This figure clearly shows that the converged K_La obtained using the data reconciliation algorithm is

significantly more precise than the precision obtained by the other methods. At lower $Q_{O_2} X / K_L a$ ratios, the standard deviation of the estimated $K_L a$ is two orders of magnitude less than three of the methods. As the ratio increases, there is significant gain in accuracy by the latter methods. This simple sensitivity analysis clearly shows that data reconciliation provides more accurate estimates of $K_L a$.

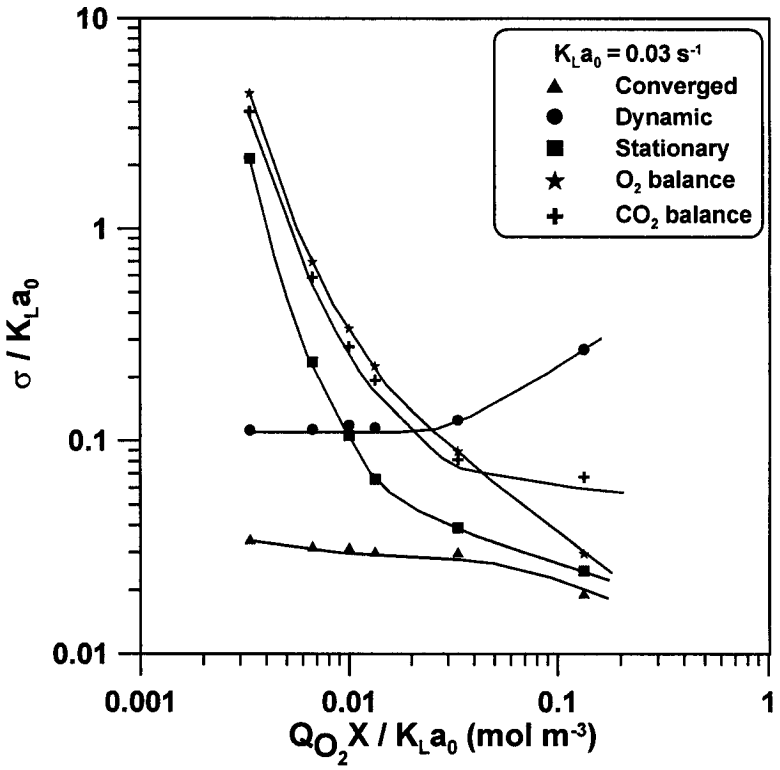

Figure 3.9 – Plot of the normalized standard deviation of the estimation of $K_L a$ as a function of $Q_{O_2} X / K_L a$ ratio for the different methods.

3.5 Conclusion

This investigation was concerned with the estimation of the overall oxygen mass transfer coefficient in viscous fermentation systems. Four different methods were available to estimate $K_L a$. However, not all four methods could be used throughout the fermentation

because when the level of dissolved oxygen becomes too low, it is not possible to use the dynamic method and one has to resort only on gas balance methods.

To get a better estimate of K_La, all available methods were solved simultaneously with a data reconciliation algorithm. The advantage of data reconciliation is the incorporation of the uncertainty in the measured variable and oxygen conservation models to provide a more reliable estimate of K_La. A sensitivity analysis showed clearly that a more accurate estimate is indeed obtained.

The value of K_La was found to vary with the type of bioreactors and time. For all fermentations conducted in the STB, K_La initially decreased, then remains constant for a period of 3 to 4 days before increasing again. This pattern is attributed to the change in viscosity due to the combined biomass growth and shear force of the mixing device. In the RPB, K_La remained relatively constant throughout the fermentation.

3.6 Nomenclature

C_L dissolved oxygen concentration (mol/m^3)

C_L^0 pseudo-steady-state dissolved oxygen concentration recorded at the initiation of the dynamic method (mol/m^3)

C_L^* dissolved oxygen concentration in equilibrium with mean gaseous oxygen concentration (mol/m^3)

C_P dissolved oxygen concentration recorded by the oxygen probe (mol/m^3)

K_La overall oxygen mass transfer coefficient (s^{-1})

J objective function

P pressure (Pa)

Q_G gas flow rate (m^3/s)

$Q_{O_2}X$ oxygen uptake rate (mol/m^3 s)

R gas constant (8.306 Pa m^3/(mol K))

RQ respiratory quotient

T temperature (K)

V_L liquid volume in the fermenter (m^3)

y gaseous mole fraction

GREEK LETTERS

α weighting factor associated to each term in the objective function

β relative weighting factor between measurements and conservation models

τ_P time constant of the dissolved oxygen probe (s)

σ standard deviation

SUBSCRIPTS

1 inlet stream

2 outlet stream

CO_2 carbon dioxide

O_2 oxygen

SYMBOLS

^ estimated values

~ corresponds to ideal or theoretical conditions

3.7 References

Atkinson, B. and F. Mavituna, "Biochemical Engineering and Biotechnology Handbook", 2e ed., Stockton Press, 337 (1991).

Brown, D. E., "Bioprocess Measurements and Control", Chem. Ind., 678 (16 Sep. 1991).

Crowe, C. M., "Observability and Redundancy of Process Data for Steady State Reconciliation", Chem. Eng. Sci. **44**, 2909 (1989).

Dorresteijn, R. C., C. D. de Gooijer, J. Tramper and E. C. Beuvery, "A Simple Dynamic Method for On-Line Determination of K_La During Cultivation of Animal Cells", Biotech. Techniques **8**, No. 9, 675-680 (1994).

Gagnon, H., M. Lounes and J. Thibault, "Power Consumption and Mass Transfer in Agitated Gas-Liquid Columns: A Comparative Study", Can. J. Chem. Eng. **76**, 379-389 (1998).

Hodouin, D., C. Bazin and S. Makni, "On-Line Reconciliation of Mineral Processing Data. Proc. of the AIME/SME Symposium - Emerging Computer Techniques for the Mineral Industry", Reno, Nevada (Feb. 1993).

Kubicek, C. P., O. Zehentgruber, H. El-Kalak and M. Röhr, "Regulation of Citric Acid Production by Oxygen Effects of Dissolved Tension on Adenylate Levels and Respiration in *Aspergillus niger*", European J. Appl. Microbiol. Biotechnol. **9**, 101-115 (1980).

Liebman, M. J., T. F. Edgar and L. S. Lasdon, "Efficient Data Reconciliation and Estimation for Dynamic Processes Using Nonlinear Programming Techniques", Computer Chem. Eng. **16**, 963 (1992).

Lounes, M. and J. Thibault, "Hydrodynamics and Power Consumption of a Reciprocating Plate Gas-Liquid Column", Can. J. Chem. Eng. **71**, 497-506 (1993).

Mah, R. S. H., "Chemical Process Structures and Information Flows", Batterworths, Boston (1990).

Makni, S., D. Hodouin and C. Bazin, "A Recursive Node Imbalance Method Incorporating a Model of Flowrate Dynamics for On-Line Material Balance of Complex Flowsheets", Mineral Eng. **8(7),** 753 (1995).

Moo-Young, M. and H. W. Blanch, "Design of Biochemical Reactors – Mass transfer Criteria for Simple and Complex Systems", In: A. Fiechter (ed.), Advances in Biochemical Engineering, Springer-Verlag, Berlin, **19**, 1 (1981).

Pouliot, K., J. Thibault, A. Garnier and G. Acuña Leiva, "K_La Evaluation During the Course of Fermentation Using Data Reconciliation Techniques", Bioprocess Eng. 23, 565-573 (2000).

Röhr, M., C. P. Kubicek and J. Kominek, "Citric acid", in: Biotechnology 1st ed. (Rehm, H.J. and G. Reed, eds.), Verlag Chemie, Weinheim, **3**, 419-454, (1983).

Romagnoli, J. A. and M. C. Sanchez, "Data Processing and Reconciliation for Chemical Process Operations", Academic Press, Toronto (2000).

Schumpe, A., I. Adler, and W. D. Deckwer, "Solubility of Oxygen in Electrolyte Solutions", Biotechnol. Bioeng. **20**, 145 (1978).

Taguchi, H. and A. E. Humphrey, "Dynamic Measurement of the Volumetric Oxygen Transfer Coefficient in Fermentation Systems", J. Ferment. **44**, 881(1966).

CHAPTER 4

PRELIMINARY RESULTS PERTAINING TO *Aspergillus niger* FERMENTATION

4.1 Introduction

The objective of Chapter 3 was to study the oxygen mass transfer in two different types of fermenters for a viscous fermentation. Only a portion of the results obtained throughout this study could be presented in the previous chapter. Other process variables were also measured throughout the fermentation. These are the concentrations of biomass, citric acid, and sugars, the pH, and the power input per unit volume. Some of these results such as the biomass concentration were partly discussed in the previous chapter. The other results are important to understand the behaviour of the microorganism *Aspergillus niger* when subjected to different types of agitation system and agitation intensity. These results are yet too partial to be published as a refereed publication but they nevertheless are an important part of the work performed in this investigation.

4.1.1 MATERIALS AND METHODS

The description and operating conditions of bioreactors used: the reciprocating plate bioreactor (RPB) and the stirred tank (STB) bioreactor were presented in Chapters 2 and 3. A sample of the fermentation broth was collected every day from each bioreactor and was analyzed for biomass, pH, citric acid and sugars. After the sample was taken, it was

immediately analyzed for pH with a Barnant 30 digital meter (Model No. 559-3810). Samples were then centrifuged at 15 000 RPM for 20 minutes and then the supernatant was filtered using a pre-weighted 45 μm Gelman filter (Gelman Sciences Inc glass fiber filter, Type A/E, 47 mm, Prod. No. 61631). The biomass was resuspended in distilled water to leach out residual sugars and nutrients, and centrifuged again. The supernatant and biomass were filtered. The filter and the biomass were placed in an oven (dryer) for 20 hours at 85-90 ^{o}C before measuring the dry weight of biomass. The method of Marier and Boulet (1958) was used to determine the citric acid concentration. Sucrose, glucose and fructose were measured by HPLC (Waters 717 Auto Sampler, Waters 486 Tuneable Absorbance Detector, Waters 410 Differential Refractometer) using an ion-exchange column (Waters, Sugar Pak column, Part No. WAT085188). Each fermentation experiment was run for duration of 12-13 days.

4.2 Results and discussion

4.2.1 BIOMASS

As explained in Chapter 3, the type of agitation and speed had a significant effect on the amount of biomass produced. A visual inspection of the samples (Appendix F.1) taken every day showed (Appendix F.1) that the morphology of microorganism in the RPB was long fibers whereas the growth of microorganism was in pellet form in the STB. The mixing system in the RPB provided a more uniform mixing and the shear on the microorganism was low compared to the STB, which was more conducive to growth. This is evidenced by the results shown in Fig. 3.2.

4.2.2 CITRIC ACID

Similar to biomass production, an increase in citric acid production is obtained with an increase in agitation speed as shown in Fig. 4.1. Even though the total production of citric acid is not significant or comparable to those reported in the literature (Röhr, 1983), the same general trend is observed. One of the reasons for the lower concentration of citric acid is due to the fluctuation of the dissolved oxygen concentration performed during the dynamic method calculation. Kubicek et al. (1980) had found that the citric acid production decreased irreversibly when aeration was ceased for few minutes. This was not considered while selecting *Aspergillus niger* fermentation for the study since the main objective of this work was not to optimize the citric acid production but to evaluate K_La using data reconciliation technique in a fermentation with a relatively slow metabolism and that leads to a viscous fermentation broth.

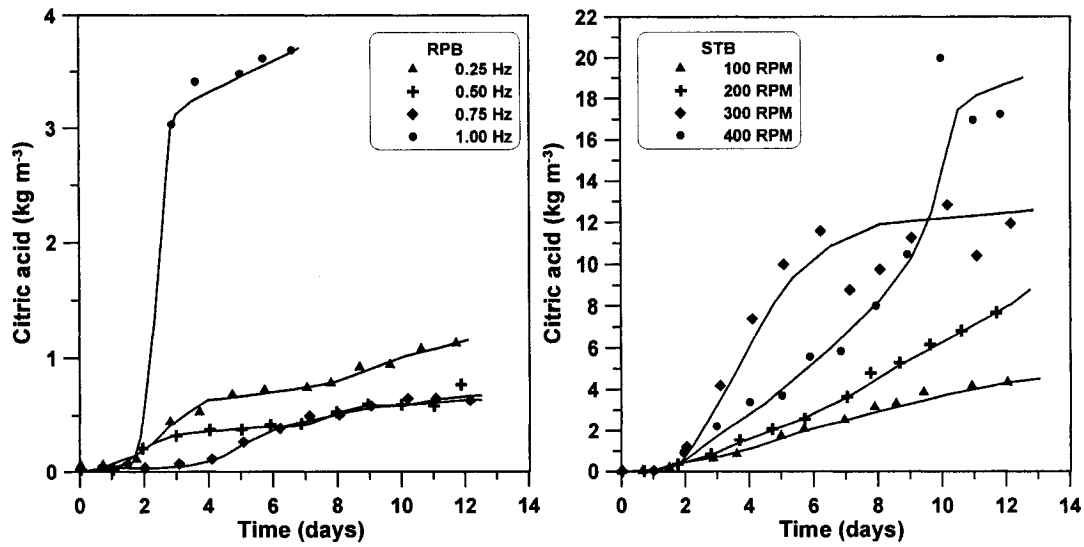

Figure 4.1 – Citric acid produced with the experiments done in the RPB and the STB at different agitation speeds.

In the RPB, the citric acid concentration increases to about 1 kg/m^3, except for frequency of 1.0 Hz where the concentration of citric acid reached approximately 3.5 kg/m^3. The

concentration of citric acid that was obtained in the STB is between 5 to 15 kg/m^3. Therefore, it was observed that although the mixing achieved in the RPB is more uniform, the citric acid production is higher in the STB. As discussed earlier, a high biomass concentration as in the RPB is associated with a lower concentration of citric acid (Röhr, 1983).

4.2.3 pH

The pH of the solution at the beginning of the experiment was around 3.6. As the fermentation progresses, the pH dropped in the RPB and the STB. During the later stages of fermentation process, the pH remained constant for the experiments conducted in the STB whereas, for experiments in the RPB, the pH was observed to increase. There is no reason yet available to explain this phenomenon. It is interesting to note that the same trend was observed for dissolved oxygen concentration profile (Fig. 3.3). More experiments need to be performed to elucidate this result.

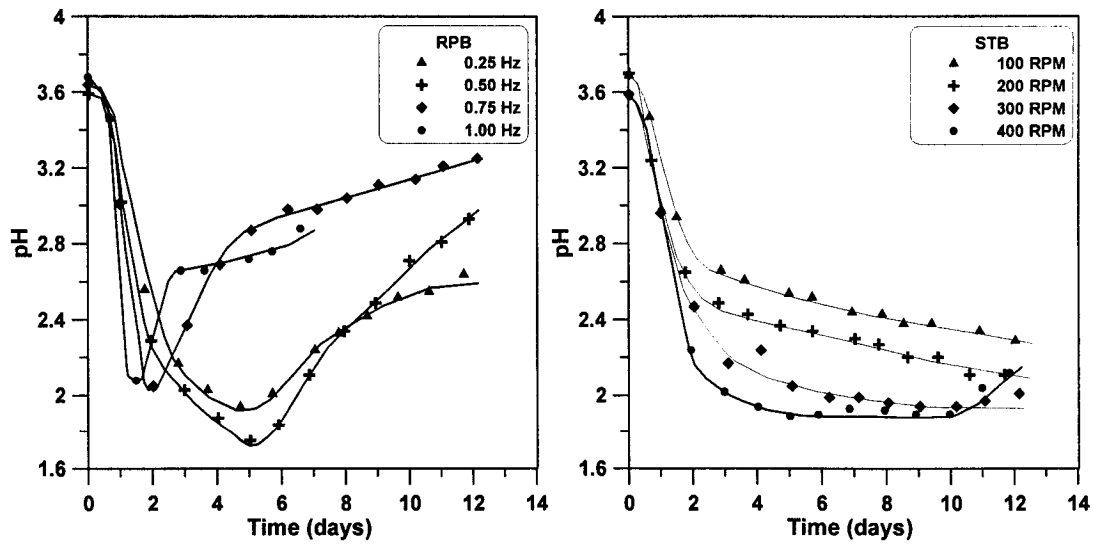

Figure 4.2 – Measured pH as a function of time for experiments conducted in the RPB and the STB at different agitation intensities.

4.2.4 POWER INPUT PER UNIT VOLUME

The power per unit volume for the experiments made in the RPB increases as the fermentation progresses whereas, in the STB, it is found to decrease slightly. The behaviour observed during experiments in the RPB is expected since the viscosity of the broth increases and thus more power is required to reciprocate the plates in the medium.

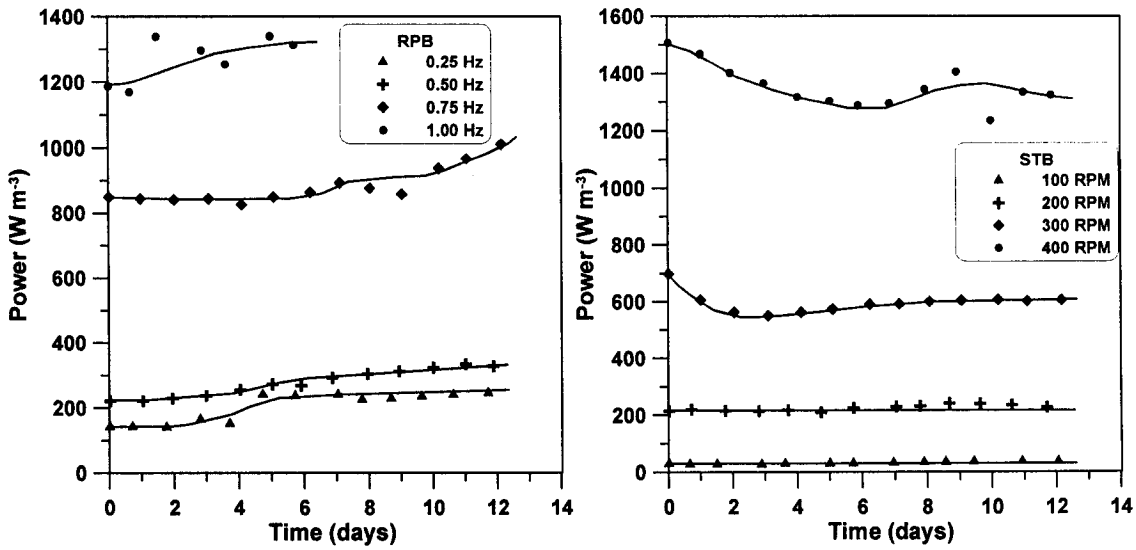

Figure 4.3 – Power input per unit volume as a function of time for experiments conducted in the RPB and the STB at different agitation intensities.

4.2.5 SUGAR COMPOSITION

Along with the bioreactors, the medium was also autoclaved before the start of the experiment. During the autoclave process, the sucrose was partially broken down into glucose and fructose as evidenced from the initial composition shown in Fig. 4.4. The consumption of sugars in the RPB was more important than the one in the STB because of the higher biomass production in the RPB as observed in Fig. 4.4 for the two experiments in the RPB and STB that had nearly the same power input per unit volume.

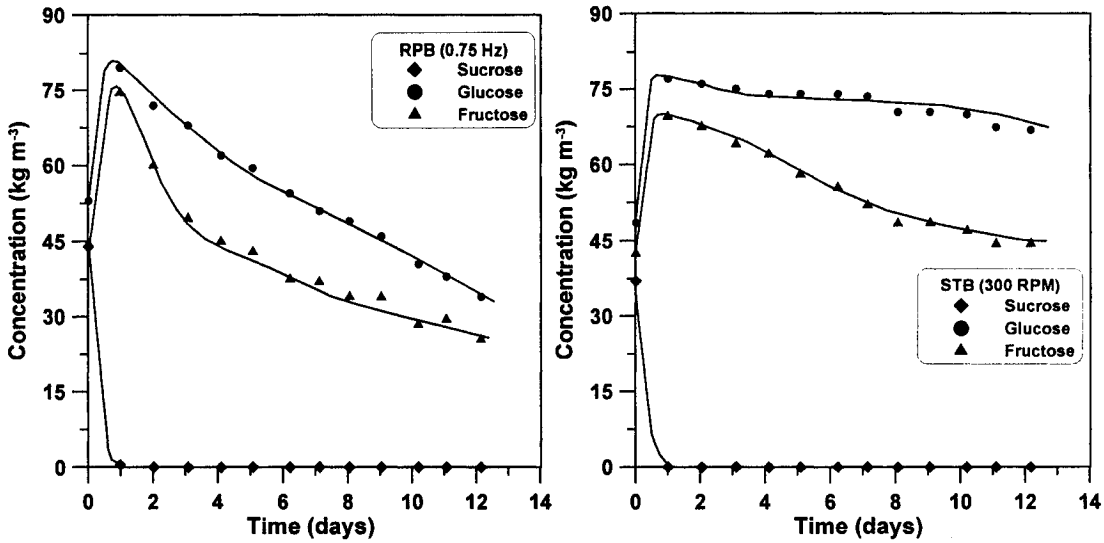

Figure 4.4 – Sugar concentration as a function of time for experiments conducted in the RPB and the STB at different agitation intensities.

4.3 Conclusion

This Chapter has presented some results obtained during fermentation experiments done to measure K_La in viscous fermentation broths. These results complement those presented in Chapter 3 and help to shed some light on the behaviour of the microorganism *Aspergillus niger*. More experiments need to be performed to better understand the impact of the type of mixing device and the intensity of agitation on the production of biomass and citric acid.

4.4 References

Atkinson, B. and F. Mavituna, "Biochemical Engineering and Biotechnology Handbook", Stockton Press **2e ed.**, p.337 (1991).

Röhr, M., C.P. Kubicek and J. Kominek; "Citric acid", in: Biotechnology 1st ed. (Rehm, H.J. and G. Reed, eds.), Verlag Chemie, Weinheim, **3**, 419-454, (1983).

Kubicek, C. P., O. Zehentgruber, H. El-Kalak and M. Röhr, Regulation of Citric Acid Production by Oxygen Effects of Dissolved Tension on Adenylate Levels and Respiration in *Aspergillus niger*, European J. Appl. Microbiol. Biotechnol. **9**, 101-115 (1980).

Marier, J.R.and M. Boulet, Direct Determination of Citric Acid in Milk with an Improved Pyridine-Acetic Anhydride Method, J. Dairy Sci. **41**, 1683-1692 (1958).

CHAPTER 5

SUMMARY & CONCLUSIONS

Experiments were performed with a model fluid (wood pulp) and microorganism *Aspergillus niger* to study viscous fermentation systems. Two types of bioreactors, a reciprocating plate bioreactor (RPB) and a stirred tank bioreactor (STB) were used for the investigation. The RPB was found to be a better mixing device compared to the STB for wood pulp system with respect to its ability to provide high oxygen mass transfer coefficient. However, the critical threshold power input per unit volume required to break the bubbles was found to be lower in case of the experiments performed in the STB. Once the critical threshold power was reached in the RPB, the K_La increased rapidly. Different coefficients of the power law equation to correlate K_La with operating conditions were obtained for different pulp concentrations. It was found that before the critical threshold is reached, K_La is a strong function of the superficial gas velocity whereas when the critical threshold is reached, it is a function of power input per unit volume. Therefore, to have a greater influence of power input per unit volume on the K_La, the bioreactor should be run at the intensity above the critical threshold value if, of course, the microorganism can tolerate high shear.

Experiments performed with *Aspergillus niger* fermentation show that the RPB was a better device for producing high biomass concentration whereas the preferred device to produce citric acid would be the STB. Due to the high biomass concentration produced during the experiments performed in the RPB, the dissolved oxygen concentration decreased rapidly below a critical value and the K_La had to be evaluated using only the gas balance

methods. The dissolved oxygen concentration for experiments performed in the STB was always higher so that all the four methods were used to calculate K_La except for the experiment performed at 100 rpm when the dissolved oxygen concentration decreased below a critical value due to low agitation intensity. For all the experiments performed, data reconciliation technique was used successfully to estimate K_La. Data reconciliation technique took into account all the measured variables and mass conservation models to calculate a unique value of K_La. A sensitivity analysis clearly showed that more reliable and accurate K_La values were obtained using a data reconciliation algorithm.

5.1 Recommendations

A dissolved oxygen probe with small time constant is required to get a good estimate of K_La. This is especially important when a high K_La is to be measured. The probe used in this study had a time constant of approximately 17 s and the membrane thickness was 50 μm. A dissolved oxygen probe with membrane thickness of 25 μm was used by other researchers with a typical time constant of the order of 5-6 s (Lounes and Thibault, 1994). However, such a membrane kit is no more available.

It was found that the STB did not produce a homogenous mixing during experiments with wood pulp solutions. Therefore, K_La should be measured at more than one location in order to obtain a better estimate of K_La.

Some attempts were made to measure the viscosity of the model fluid in order to correlate the oxygen mass transfer coefficient with this variable. It was not possible to determine the viscosity using conventional viscometers since water was expelled from the pulp solution to form a solid mass and it was impossible to have a homogenous solution during the test. New

methods are required to evaluate this important parameter in order to relate the K_La obtained from wood pulp solutions and actual *Aspergillus niger* fermentation.

5.2 Reference

Lounes, M. and J. Thibault, "Mass Transfer in a Reciprocating Plate Bioreactor" Bioprocess Eng. 13, 169-189 (1994).

APPENDIX

A.1 Experimental results with wood pulp in the STB.

		Superficial Gas Velocity							
		0.0020 m/s		0.0041 m/s		0.0081 m/s		0.0122 m/s	
Pulp (kg/m^3)	Agitation (RPM)	Power / Volume (W/m^3)	K_La (s^{-1})	Power / Volume (W/m^3)	K_La (s^{-1})	Power / Volume (W/m^3)	K_La (s^{-1})	Power / Volume (W/m^3)	K_La (s^{-1})
4.12	50	1.32	0.00320	1.56	0.00441	1.96	0.00641	2.61	0.01113
	100	31.18	0.00371	28.05	0.00489	28.34	0.00750	26.80	0.01143
	200	262.68	0.00589	271.87	0.00885	227.96	0.01547	186.62	0.01987
	300	900.36	0.01288	803.02	0.02136	624.72	0.03072	535.48	0.03834
	400	2044.45	0.02482	1896.47	0.04225	1507.84	0.05961	1257.84	0.06231
2.94	50	0.93	0.00369	0.90	0.00430	1.27	0.00703	2.72	0.01108
	100	27.66	0.00372	26.05	0.00455	23.41	0.00767	24.97	0.01155
	200	252.30	0.00548	249.00	0.00969	194.58	0.01554	166.39	0.02121
	300	850.38	0.01538	807.44	0.02160	589.24	0.02912	481.99	0.04241
	400	1992.59	0.03139	1835.78	0.03612	1495.92	0.06588	1194.12	0.06386
1.47	50	9.91	0.00287	9.13	0.00430	9.72	0.00703	11.25	0.01108
	100	38.46	0.00354	41.25	0.00442	39.15	0.00707	34.89	0.01141
	200	241.63	0.00517	230.71	0.00969	195.56	0.01554	176.38	0.02075
	300	864.04	0.01490	807.43	0.02160	691.46	0.02912	533.10	0.03825
	400	3178.65	0.03139	1859.68	0.03754	1484.34	0.06588	1179.64	0.06417
0 (Water)	50	3.07	0.00176	4.16	0.00322	5.12	0.00699	5.20	0.01040
	100	28.14	0.00218	21.74	0.00358	27.35	0.00716	28.23	0.01100
	200	210.49	0.00803	184.13	0.01080	162.30	0.01440	160.07	0.01790
	300	722.48	0.01890	593.63	0.02570	462.89	0.02630	414.42	0.03520
	400	1617.73	0.03098	1430.26	0.03700	1155.38	0.05456	1023.59	0.06462

B.1 Experimental results with wood pulp in the RPB.

		Superficial Gas Velocity							
		0.0020 m/s		0.0041 m/s		0.0081 m/s		0.0122 m/s	
Pulp (kg/m^3)	Agitation (Hz)	Power / Volume (W/m^3)	K_La (s^{-1})	Power / Volume (W/m^3)	K_La (s^{-1})	Power / Volume (W/m^3)	K_La (s^{-1})	Power / Volume (W/m^3)	K_La (s^{-1})
4.12	0.10	6.10	0.00231	8.19	0.00357	9.84	0.00754	12.47	0.00914
	0.25	39.61	0.00208	41.38	0.00521	49.41	0.00893	57.06	0.01445
	0.50	223.04	0.00251	232.75	0.00455	238.97	0.00965	280.88	0.01481
	0.75	707.10	0.00607	699.37	0.01027	700.69	0.01934	728.46	0.03088
	1.00	1530.87	0.01710	1592.22	0.02651	1533.46	0.05413	1477.29	0.06647
	1.25	2706.40	0.02750	2684.81	0.05779	2577.12	0.09540	2509.93	0.15960
2.94	0.10	5.54	0.00210	6.16	0.00449	7.38	0.00888	8.63	0.01412
	0.25	35.08	0.00220	42.13	0.00562	45.49	0.01177	54.29	0.01996
	0.50	221.66	0.00381	219.93	0.00712	218.96	0.01249	235.63	0.02323
	0.75	652.06	0.01116	677.51	0.01702	663.25	0.03079	662.16	0.04760
	1.00	1406.53	0.02164	1439.32	0.03236	1371.31	0.06931	1405.97	0.09874
	1.25	2633.03	0.03348	2566.09	0.08776	2499.26	0.14070	2438.21	0.19070
1.47	0.10	4.88	0.00228	6.18	0.00477	8.46	0.00998	10.50	0.01475
	0.25	32.86	0.00255	36.78	0.00475	43.76	0.00945	52.82	0.01504
	0.50	204.66	0.00341	199.43	0.00649	220.44	0.01288	236.69	0.02016
	0.75	685.54	0.00902	660.75	0.01664	687.98	0.03017	722.53	0.04338
	1.00	1461.50	0.02393	1456.44	0.03848	1371.88	0.08536	1486.15	0.13510
	1.25	2762.91	0.05237	2593.25	0.12550	2530.74	0.22550	2550.56	0.34240
0 (Water)	0.10	5.24	0.00309	7.76	0.00585	9.79	0.01180	10.84	0.01532
	0.25	35.85	0.00359	40.01	0.00625	52.78	0.01520	61.01	0.02080
	0.50	213.63	0.00584	222.54	0.01112	244.12	0.02352	271.50	0.03449
	0.75	743.71	0.01326	712.60	0.03430	735.51	0.06920	757.50	0.11720
	1.00	1499.07	0.03920	1397.04	0.07930	1513.79	0.15250	1480.03	0.28800
	1.25	2701.24	0.05400	2656.69	0.22100	2577.07	0.36850	2551.15	0.61610

C.1 Data reconciliation program

The data reconciliation program was written in FORTRAN. The listing of the main program and the Gaussien subroutine is given. The optimization subroutines were obtained from Harwell Library (A. BARRAUD and P. LAPORTE, 1989).

C.1.1 MAIN PROGRAM

```
 PROGRAM RECON
C*************************************************************
    INTEGER NPA,MCON,KEG,IPRINT,LP,K,LWRITE
    INTEGER IPRINT1,LP1,MODE1,METSOL
    INTEGER MAXITN,IH,IERR,MODE,LSEC(3),ITER
    DOUBLE PRECISION ACC,W(5000),F,C(20),F1,G(20),SCA(20)
    DOUBLE PRECISION PA(20),PAP(20),X(6,10000),VAL0(20),PON(20),FF(20)
    DOUBLE PRECISION DPAR,VAR(7,10000),FCON,PACON(20),SDEV(7)
        DOUBLE PRECISION KLAVAR(7,10000),AVG(7),DKLA
    CHARACTER*13 FICHIER
    EXTERNAL MODEL

    COMMON /MO/X,PON,FF,VAL0,PA,LSEC,LWRITE
    COMMON /VA13B/IPRINT,LP,MAXFUN,MODE,NFUN
    COMMON /VF04DD/IPRINT1,LP1,MAXITN,IH,IERR,MODE1

    IPRINT=0
    IPRINT1=0
    MAXITN=500
    IH=-3

    OPEN (4,FILE='KLA1004.DAT')
        ILOOPMAX=1000
        DO 200 ILOOP=1,ILOOPMAX

    NPA=15
        ITYPE=2
        IF (ITYPE .EQ .1) THEN
     CALL ENTREDON_1
        ELSE
         LWRITE=1
     OPEN (3,FILE='SimDat.dat')
         CALL SIMMODEL
         LWRITE=0
         CLOSE(3)
        END IF

    OPEN (1,FILE='recon1.dat')
    OPEN (2,FILE='recon2.dat')
    OPEN (3,FILE='recon3.dat')

    DO 10 I=1,NPA
```

```
      PA(I)=VAL0(I)
      PAP(I)=1.
   10 CONTINUE

      LWRITE=0
      METSOL=1
      ACC=1.0D-08

      FCON=1.0E+30
      ITER=0

      DO 15 I=1,NPA
        SCA(I)=0.1
   15 CONTINUE

      IF (METSOL .EQ. 1) THEN
   20 CONTINUE
        ITER=ITER+1
        CALL MODEL(NPA,PAP,F,C)
C       PRINT *,ILOOP,ITER,F

            IF (F .LT. FCON) THEN
              FCON=F
              DO 19 J=1,NPA
                PACON(J)=PAP(J)
   19       CONTINUE
        END IF

        DO 30 I=1,NPA
          CALL MODEL(NPA,PAP,F,C)
          DPAR=ABS(PAP(I)*.01/FLOAT(ITER))
          PAP(I)=PAP(I)+DPAR
          CALL MODEL(NPA,PAP,F1,C)

              IF (F1 .LT. FCON) THEN
                FCON=F1
                DO 18 J=1,NPA
                  PACON(J)=PAP(J)
   18         CONTINUE
          END IF

          G(I)=(F1-F)/DPAR
          PAP(I)=PAP(I)-DPAR
   30   CONTINUE
        CALL VA13A(NPA,PAP,F,G,SCA,ACC,W,LINK)
        IF((LINK .NE. 2) .AND. (ITER .LE. MAXITN)) GOTO 20

      ELSEIF (METSOL .EQ. 2) THEN
        MCON=NPA
        KEG=0
        CALL VF04AD(MODEL,NPA,MCON,KEG,PAP,F,ACC,W)

      ELSEIF (METSOL .EQ. 3) THEN
        CALL MODEL(NPA,PAP,F,C)
        DO 40 J=1,1000
          DO 35 I=1,12
```

```
      CALL GAUSSIEN(SIGMA)
      PA(I)=VAL0(I)+SIGMA/(PON(I)*3.)
      PAP(I)=PA(I)/VAL0(I)
35    CONTINUE
     CALL MODEL(NPA,PAP,F,C)
     VAR(1,J)=SQRT(FF(13))
     VAR(2,J)=SQRT(FF(14))
     VAR(3,J)=PA(13)-SQRT(FF(15))
     VAR(4,J)=PA(13)-SQRT(FF(16))
     VAR(5,J)=PA(13)-SQRT(FF(17))
     VAR(6,J)=PA(15)-SQRT(FF(18))
     WRITE (2,101) (VAR(I,J),I=1,6)
40  CONTINUE
   CALL VARIANCE(6,1000,VAR,SDEV,AVG)
   STOP
  ELSE
    STOP
  END IF

  LWRITE=0
       DO 17 J=1,NPA
        PAP(J)=PACON(J)
17 CONTINUE

  CALL MODEL(NPA,PAP,F,C)

  KLAVAR(1,ILOOP)=PA(13)
       KLAVAR(2,ILOOP)=PA(14)/(PA(15)-PA(5))
  KLAVAR(3,ILOOP)=(1./(PA(6)*(PA(15)-PA(5))))*(PA(1)*PA(8)/(8.313*
 1     PA(2)))*(PA(9)-PA(10))
  KLAVAR(4,ILOOP)=(1./(PA(6)*(PA(15)-PA(5))))*(PA(1)*PA(8)/(8.313*
 1     PA(2)))*(1./PA(7))*(PA(12)-PA(11))

  KLAVAR(5,ILOOP)=VAL0(13)
  KLAVAR(6,ILOOP)=VAL0(14)

       CALL KLADYNA(DKLA)
  KLAVAR(7,ILOOP)=DKLA


  PRINT *, ILOOP,(KLAVAR(I,ILOOP),I=1,7)
  WRITE(4,101) FLOAT(ILOOP),(KLAVAR(I,ILOOP),I=1,7)
  CLOSE (1)
  CLOSE (2)
  CLOSE (3)

200 CONTINUE

  CALL VARIANCE(7,ILOOPMAX,KLAVAR,SDEV,AVG)
       PRINT *, (SDEV(I),I=1,7)
  WRITE(4,101)
  WRITE(4,101) (AVG(I),I=1,7)
  WRITE(4,101) (SDEV(I),I=1,7)
       CLOSE(4)

101 FORMAT(15E12.4)
```

```
      END
C*************************************************************
      SUBROUTINE MODEL(N,PAP,F,C)

      INTEGER N,K,LSEC(3),LWRITE
      DOUBLE PRECISION PA(20),PAP(20),VAL0(20),PON(20),FF(20),FAC
      DOUBLE PRECISION X(6,10000),F,C(20)

      COMMON /MO/X,PON,FF,VAL0,PA,LSEC,LWRITE

      DO 15 I=1,N
       PA(I)=PAP(I)*VAL0(I)
   15 CONTINUE

      FF(1)=(VAL0(1)-PA(1))**2
      PON(1)=1./3000.

      FF(2)=(VAL0(2)-PA(2))**2
      PON(2)=1./1.

      FF(3)=(VAL0(3)-PA(3))**2
      PON(3)=1./2.

      FF(4)=(VAL0(4)-PA(4))**2
      PON(4)=1./0.00625

      SUM=0.
      DO 10 I=1,LSEC(1)-1
       SUM=SUM+X(2,I)
       IF (LWRITE .EQ. 1) THEN
        WRITE(3,101)(X(1,I+1)-X(1,1)),X(2,I+1),PA(5),PA(5)
       ENDIF
   10 CONTINUE

      FF(5)=(SUM/FLOAT(LSEC(1)-1)-PA(5))**2
      PON(5)=1./0.00625

      FF(6)=(VAL0(6)-PA(6))**2
      PON(6)=1./0.0001

      FF(7)=(VAL0(7)-PA(7))**2
      PON(7)=1./0.2

      FF(8)=(VAL0(8)-PA(8))**2
      PON(8)=1./1.66D-06

      FF(9)=(VAL0(9)-PA(9))**2
      PON(9)=1./0.001

      FF(10)=(VAL0(10)-PA(10))**2
      PON(10)=1./0.002

      FF(11)=(VAL0(11)-PA(11))**2
      PON(11)=1./0.0005
```

```
      FF(12)=(VAL0(12)-PA(12))**2
      PON(12)=1./0.001

      CP1=PA(5)
      CL1=CP1
      T0=X(1,LSEC(1))
      TGAZ1=7.
      SUM1=0.
      DO 12 I=LSEC(1),LSEC(2)-1
       NDT=100
       DT=X(1,I+1)-X(1,I)
       DTT=DT/FLOAT(NDT)
       DO 11 J=1,NDT
        TIME=X(1,I)-T0+DTT*FLOAT(J)
        IF (CL1 .LE. .02) THEN
         FAC=CL1/(.06+CL1)
        ELSE
         FAC=1.
        ENDIF
        CL2=CL1+DTT*(PA(13)*EXP(-TIME/TGAZ1)*(PA(15)-CL1)-PA(14)*FAC)
        IF (CL2 .LE. 0.) CL2=0.
        CP2=CP1+(DTT/PA(3))*(CL1-CP1)
        IF (CP2 .LE. 0.) CP2=0.
        CP1=CP2
        CL1=CL2
   11   CONTINUE
       SUM1=SUM1+(X(2,I+1)-CP1)**2
       IF (LWRITE .EQ. 1) THEN
        WRITE(3,101) (X(1,I+1)-X(1,1)),X(2,I+1),CL1,CP1
       ENDIF
   12  CONTINUE
  101  FORMAT(10E13.5)

      FF(13)=SUM1/FLOAT(LSEC(2)-LSEC(1)-1)

      TGAZ2=1.5
      T0=X(1,LSEC(2))
      SUM2=0.
      DO 14 I=LSEC(2),LSEC(3)-1
       NDT=100
       DT=X(1,I+1)-X(1,I)
       DTT=DT/FLOAT(NDT)
       DO 13 J=1,NDT
        TIME=X(1,I)-T0+DTT*FLOAT(J)
        IF (CL1 .LE. .02) THEN
         FAC=CL1/(.06+CL1)
        ELSE
         FAC=1.
        ENDIF
        CL2=CL1+DTT*(PA(13)*(1-EXP(-TIME/TGAZ2))*(PA(15)-CL1)
     1      -PA(14)*FAC)
        IF (CL2 .LE. 0.) CL2=0.
        CP2=CP1+(DTT/PA(3))*(CL1-CP1)
        IF (CP2 .LE. 0.) CP2=0.
        CP1=CP2
```

```
      CL1=CL2
   13 CONTINUE
      SUM2=SUM2+(X(2,I+1)-CP1)**2
      IF (LWRITE .EQ. 1) THEN
       WRITE(3,101) (X(1,I+1)-X(1,1)),X(2,I+1),CL1,CP1
      ENDIF
   14 CONTINUE

      FF(14)=SUM2/FLOAT(LSEC(3)-LSEC(2)-1)

      FF(15)=(PA(13)-PA(14)/(PA(15)-PA(5)))**2

      FF(16)=(PA(13)-((1./(PA(6)*(PA(15)-PA(5))))*(PA(1)*PA(8)/(8.313*
     1     PA(2)))*(PA(9)-PA(10))))**2

      FF(17)=(PA(13)-((1./(PA(6)*(PA(15)-PA(5))))*(PA(1)*PA(8)/(8.313*
     1     PA(2)))*(1./PA(7))*(PA(12)-PA(11))))**2

      FF(18)=(PA(15)-PA(4)*((PA(9)+PA(10))/(2.*0.2094))
     1     *(PA(1)/101300.))**2

      F=0.
      DO 20 I=1,18
       F=F+FF(I)*(PON(I)*3.)**2
C      PRINT *, I,F,PA(I),VAL0(I),FF(I),PON(I)
   20 CONTINUE

      DO 30 I=1,N
       C(I)=PAP(I)
   30 CONTINUE
      RETURN
      END


C ********************************************

      SUBROUTINE VARIANCE(IC,IR,VAR,SDEV,AVG)

      INTEGER IC,IR
      DOUBLE PRECISION VAR(7,10000),MIN,MAX,SUM1,SUM2
           DOUBLE PRECISION SDEV(7),AVG(7)

      DO 100 I=1,IC
       SUM1=0.
       MAX=-1.D+30
       MIN=1.D+30
       DO 50 J=1,IR
        SUM1=SUM1+VAR(I,J)
        IF (VAR(I,J) .LT. MIN) MIN=VAR(I,J)
        IF (VAR(I,J) .GT. MAX) MAX=VAR(I,J)
   50  CONTINUE
       AVG(I)=SUM1/FLOAT(IR)
       SUM2=0.
       DO 60 J=1,IR
        SUM2=SUM2+(VAR(I,J)-AVG(I))**2
   60  CONTINUE
```

```
      VARIAN=SUM2/FLOAT(IR-1)
      SDEV(I)=SQRT(VARIAN)
C       PRINT *, I+12,MIN,MAX,AVG(I),VARIAN,SDEV(I),1./(3.*SDEV(I))
  100 CONTINUE
      RETURN
      END


C*************************************************************

      SUBROUTINE SIMMODEL

      INTEGER N,K,LSEC(3),LWRITE
      DOUBLE PRECISION PA(20),PAP(20),VAL0(20),PON(20),FF(20),FAC
      DOUBLE PRECISION X(6,10000),F,C(20),VALKLA,QO2X,RQ,VAR(7,10000)
           DOUBLE PRECISION SDEV(7),AVG(7)

      COMMON /MO/X,PON,FF,VAL0,PA,LSEC,LWRITE

      NPA=15
           VALKLA=.03
           QO2X=0.0004
           RQ=1.0

      VAL0(1)=101300.
      PON(1)=1./3000.

      VAL0(2)=30.+273.2
      PON(2)=1./1.

      VAL0(3)=15.
      PON(3)=1./2.

      VAL0(4)=0.97*7.7/32.
      PON(4)=1./0.00625

      VAL0(5)=VAL0(4)-QO2X/VALKLA
      PON(5)=1./0.00625
           print *, val0(5)

      VAL0(6)=18./1000.
      PON(6)=1./0.0001

      VAL0(7)=RQ
      PON(7)=1./0.2

      VAL0(8)=10./(1000.*60.)
      PON(8)=1./1.66D-06

      VAL0(9)=0.2095
      PON(9)=1./0.001

      VAL0(10)=VAL0(9)-VALKLA*VAL0(6)*(VAL0(4)-VAL0(5))*(8.313*
     1     VAL0(2))/(VAL0(1)*VAL0(8))
      PON(10)=1./0.001
```

```
      VAL0(11)=0.0003
      PON(11)=1./0.0003

      VAL0(12)=VAL0(11)+VALKLA*VAL0(6)*(VAL0(4)-VAL0(5))*RQ*(8.313*
     1     VAL0(2))/(VAL0(1)*VAL0(8))
      PON(12)=1./0.001

      VAL0(13)=VALKLA
           VAL0(14)=QO2X
           VAL0(15)=VAL0(4)

      CP1=VAL0(5)
      CL1=CP1
      T0=0.
           X(1,1)=0.

           DO 9 I=1,10
            X(1,I)=FLOAT(I-1)*20.
            X(2,I)=VAL0(5)
C          PRINT *, I,X(1,I),X(2,I)
    9 CONTINUE
      LSEC(1)=10

      TGAZ1=7.
           T0=X(1,LSEC(1))
      DO 12 I=LSEC(1),10000
       NDT=200
       DT=20.
       DTT=DT/FLOAT(NDT)
       DO 11 J=1,NDT
        TIME=X(1,I)+DTT*FLOAT(J)
        IF (CL1 .LE. .02) THEN
         FAC=CL1/(.06+CL1)
        ELSE
         FAC=1.
        ENDIF
        CL2=CL1+DTT*(VALKLA*EXP(-(TIME-T0)/TGAZ1)
     +              *(VAL0(4)-CL1)-QO2X*FAC)
        IF (CL2 .LE. 0.) CL2=0.
        CP2=CP1+(DTT/VAL0(3))*(CL1-CP1)
        IF (CP2 .LE. 0.) CP2=0.
        CP1=CP2
        CL1=CL2
    11  CONTINUE
       X(1,I+1)=TIME
            X(2,I+1)=CP1
C          PRINT *, I,X(1,I),X(2,I)
       LSEC(2)=I+1
            IF (CP1 .LE. 0.2*VAL0(4)) GOTO 17
    12 CONTINUE
    17 CONTINUE
   101 FORMAT(10E13.5)

           TGAZ2=1.5
      T0=X(1,LSEC(2))
           IJ=INT(1./(VALKLA*DT))
```

```
      DO 14 I=LSEC(2),5*IJ+LSEC(2)
       NDT=100
       DTT=DT/FLOAT(NDT)
       DO 13 J=1,NDT
        TIME=X(1,I)+DTT*FLOAT(J)
        IF (CL1 .LE. .02) THEN
         FAC=CL1/(.06+CL1)
        ELSE
         FAC=1.
        ENDIF
        CL2=CL1+DTT*(VALKLA*(1-EXP(-(TIME-T0)/TGAZ2))*(VAL0(4)-CL1)
     1      -QO2X*FAC)
        IF (CL2 .LE. 0.) CL2=0.
        CP2=CP1+(DTT/VAL0(3))*(CL1-CP1)
        IF (CP2 .LE. 0.) CP2=0.
        CP1=CP2
        CL1=CL2
   13  CONTINUE
       X(1,I+1)=TIME
            X(2,I+1)=CP1
C          PRINT *, I,X(1,I),X(2,I)
            LSEC(3)=I+1
   14 CONTINUE

      DO 31 I=1,12
       CALL GAUSSIEN(SIGMA)
       VAL0(I)=VAL0(I)+SIGMA/(PON(I)*3.)
   31 CONTINUE
C     IF (VAL0(10) .GT. VAL0(9)) VAL0(10)=VAL0(9)-.00001
C     IF (VAL0(12) .LT. VAL0(11)) VAL0(12)=VAL0(11)+0.00001

C MODIFICATION OF SOME PARAMETERS
      CALL GAUSSIEN(SIGMA)
      VAL0(13)=VALKLA*(1.+0.0*SIGMA)
      CALL GAUSSIEN(SIGMA)
           VAL0(14)=QO2X*(1.+0.0*SIGMA)
      CALL GAUSSIEN(SIGMA)
           VAL0(3)=VAL0(3)*(1.+0.0*SIGMA)

      DO 32 I=1,NPA
       PA(I)=VAL0(I)
            PAP(I)=1.
   32 CONTINUE

      CALL MODEL(NPA,PAP,F,C)
      DO 40 J=1,1000
       DO 35 I=1,12
        CALL GAUSSIEN(SIGMA)
        PA(I)=VAL0(I)+SIGMA/(PON(I)*3.)
        PAP(I)=PA(I)/VAL0(I)
   35  CONTINUE
       CALL MODEL(NPA,PAP,F,C)
       VAR(1,J)=SQRT(FF(13))
       VAR(2,J)=SQRT(FF(14))
       VAR(3,J)=PA(13)-SQRT(FF(15))
       VAR(4,J)=PA(13)-SQRT(FF(16))
```

```
      VAR(5,J)=PA(13)-SQRT(FF(17))
      VAR(6,J)=PA(15)-SQRT(FF(18))
   40 CONTINUE
      CALL VARIANCE(6,1000,VAR,SDEV,AVG)

      FACMODEL=1.
           DO 33 I=1,6
      PON(12+I)=FACMODEL/(3.*SDEV(I))
   33 CONTINUE

      DO 36 I=1,LSEC(3)
      CALL GAUSSIEN(SIGMA)
           X(2,I)=X(2,I)+SIGMA/(PON(5)*3.)
      IF (LWRITE .EQ. 1) THEN
       WRITE(3,101) X(1,I),X(2,I)
      ENDIF
   36 CONTINUE

      RETURN
      END


C*************************************************************

      SUBROUTINE KLADYNA(DKLA)

      INTEGER LSEC(3),LWRITE,I
      DOUBLE PRECISION PA(20),VAL0(20),PON(20),FF(20)
      DOUBLE PRECISION X(6,10000),F,C(20),DKLA,XX,YY

      COMMON /MO/X,PON,FF,VAL0,PA,LSEC,LWRITE

           II=LSEC(2)+(LSEC(3)-LSEC(2))/5
           JJ=LSEC(3)-(LSEC(3)-LSEC(2))/3

           SUM=0.
           DO 16 I=1,4
      SUM=SUM+X(2,LSEC(2)+1-I)
   16 CONTINUE
      YMIN=SUM/FLOAT(4)

           SUM=0.
           DO 15 I=1,5
      SUM=SUM+X(2,LSEC(3)+1-I)
   15 CONTINUE
      YMAX=SUM/FLOAT(5)

           A11=FLOAT(JJ-II+1)
           A12=0.
           A22=0.
           A13=0
           A23=0.
      DO 14 I=II,JJ
            XX=(X(1,I)-X(1,LSEC(2)))
            YY=1-(X(2,I)-YMIN)/(YMAX-YMIN)
            IF (YY .LE. 0.) THEN
```

```
          A11=A11-1.
         ELSE
          YY=LOG(YY)
          A12=A12+XX
          A22=A22+XX**2
          A13=A13+YY
          A23=A23+XX*YY
         END IF
  14 CONTINUE
    DKLA=-(A13*A12-A23*A11)/(A12*A12-A22*A11)

    RETURN
    END


C ********************************************

    SUBROUTINE ENTREDON_1

C VAL0  1   PRESSION (PA)
C       2   TEMPERATURE (K)
C       3   CONSTANTE DE TEMPS DE L'ELECTRODE (S)
C       4   C*L EN EQUILIBRE AVEC L'AIR  (MOL/M**3)
C       5   CL EN STATIONNAIRE AVANT LE CHANGEMENT  (MOL/M**3)
C       6   VOLUME DE LIQUIDE (M**3)
C       7   RQ (-)
C       8   DEBIT DE GAZ (M**3/S)
C       9   CONCENTRATION D'OXYGENE A L'ENTREE (FRACTION MOLAIRE)
C      10   CONCENTRATION D'OXYGENE A LA SORTIE (FRACTION MOLAIRE)
C      11   CONCENTRATION DE CO2 A L'ENTREE (FRACTION MOLAIRE)
C      12   CONCENTRATION DE CO2 A LA SORTIE (FRACTION MOLAIRE)
C      13   KLA (S-1)
C      14   QO2X (MOL/(M**3 S))
C      15   C*L EN CONDITION DE FERMENTATION (MOL/(M**3)

    INTEGER LSEC(3),LWRITE,NTEST
    DOUBLE PRECISION VAL0(20),PON(20),X(6,10000),FF(20)
         DOUBLE PRECISION FACMODEL,PA(20)
    CHARACTER*25 FICHIER
         CHARACTER*13 DRIV
    COMMON /MO/X,PON,FF,VAL0,PA,LSEC,LWRITE

    VAL0(1)=101300.
    VAL0(2)=30.+273.2
    VAL0(3)=17.
    VAL0(4)=0.97*7.7/32.

    DRIV='E:\NilRecon-1\'

    NTEST=1
    GOTO (1,2,3,4,5,6,7,8,9,10,11,12,13,14,15) NTEST
    STOP
   1 CONTINUE
    FICHIER=DRIV//'stb4kla2.prn'
    VAL0(5)=(80.8/100.)*7.7/32.
    VAL0(6)=17.14/1000.
```

```
      VAL0(7)=1.0
      VAL0(8)=10./(1000.*60.)
      VAL0(9)=.2095
      VAL0(10)=.2088
      VAL0(11)=.00035
      VAL0(12)=.0006
      VAL0(13)=.003
      VAL0(14)=4.245D-05
      VAL0(15)=VAL0(4)*((VAL0(9)+VAL0(10))/(2*0.2094))*(VAL0(1)/101300.)
      LSEC(1)=8
      LSEC(2)=160
      LSEC(3)=415

      FACMODEL=1.
      PON(13)=286.4*FACMODEL
      PON(14)=837.3*FACMODEL
      PON(15)=5419.*FACMODEL
      PON(16)=64.9*FACMODEL
      PON(17)=144.6*FACMODEL
      PON(18)=177.0*FACMODEL
      GOTO 99
.
.
.
   15 CONTINUE
      FICHIER='test4_15.txt'
      VAL0(5)=5.44/32.
      VAL0(6)=19.1/1000.
      VAL0(7)=1.2
      VAL0(8)=10./(1000.*60.)
      VAL0(9)=.2092
      VAL0(10)=.1952
      VAL0(11)=.0005
      VAL0(12)=.02293
      VAL0(13)=.0694
      VAL0(14)=0.00279
      VAL0(15)=VAL0(4)*((VAL0(9)+VAL0(10))/(2*0.209))*(VAL0(1)/101300.)
      LSEC(1)=15
      LSEC(2)=25
      LSEC(3)=59

      FACMODEL=1.
      PON(13)=225.8*FACMODEL
      PON(14)=1964.*FACMODEL
      PON(15)=167.8*FACMODEL
      PON(16)=55.1*FACMODEL
      PON(17)=39.7*FACMODEL
      PON(18)=183.*FACMODEL
      GOTO 99
   99 CONTINUE
      OPEN (1,FILE=FICHIER)
      DO 60 K=1,2000
        READ(1,*,END=100) X(1,K),X(3,K),X(2,K)
            print *, X(1,K),X(3,K),X(2,K)
        X(1,K)=X(1,K)*60.
        X(2,K)=(X(2,K)/100.)*7.7/32.
```

```
 60 CONTINUE
100 CLOSE(1)
    RETURN
    END
```

C.1.2 SUBROUTINE GAUSSIEN

```
SUBROUTINE GAUSSIEN(ECARTTYPE)
C
C ***************************************************
C * Calcul l'ecart-type et le bruit apres RETURN    *
C ***************************************************
C
    INTEGER ILOW
    REAL ECARTTYPE,SUM,DSIGMA,Z,RANDU,PI
C
    PI=3.141592654
    Z=RAND(0)
    IF (Z .LE. 0.00003) THEN
      ECARTTYPE= -4.
    ELSE IF (Z .GE. 0.99997) THEN
      ECARTTYPE = 4.
    ELSE
      DSIGMA = .05
      IF (Z .LT. .0013) THEN
         EcartType = -4.
         ILOW = 0
         SUM = .00003
      ELSE IF (Z .LT. .0062) THEN
         EcartType = -3.
         ILOW = 20
         SUM = .0013
      ELSE IF (Z .LT. .0228) THEN
         EcartType = -2.5
         ILOW = 30
         SUM = .0062
      ELSE IF (Z .LT. .0668) THEN
         EcartType = -2.
         ILOW = 40
         SUM = .0228
      ELSE IF (Z .LT. .1587) THEN
         EcartType = -1.5
         ILOW = 50
         SUM = .0668
      ELSE IF (Z .LT. .3085) THEN
         EcartType = -1.
         ILOW = 60
         SUM = .1587
      ELSE IF (Z .LT. .5) THEN
         EcartType = -.5
         ILOW = 70
         SUM = .3085
      ELSE IF (Z .LT. .6915) THEN
         EcartType = 0.
         ILOW = 80
```

```
          SUM = .5
        ELSE IF (Z .LT. .8413) THEN
          EcartType = .5
          ILOW = 90
          SUM = .6915
        ELSE IF (Z .LT. .9332) THEN
          EcartType = 1.
          ILOW = 100
          SUM = .8413
        ELSE IF (Z .LT. .9772) THEN
          EcartType = 1.5
          ILOW = 110
          SUM = .9332
        ELSE IF (Z .LT. .9938) THEN
          EcartType = 2.
          ILOW = 120
          SUM = .9772
        ELSE IF (Z .LT. .9987) THEN
          EcartType = 2.5
          ILOW = 130
          SUM = .9938
        ELSE IF (Z .LT. .99997) THEN
          EcartType = 3.
          ILOW = 140
          SUM = .9987
        ELSE
          STOP
       END IF
       DO 80 II = ILOW,160
       SUM = SUM+(EXP(-((ABS(ECARTTYPE)+DSIGMA/2)**2./2.))/SQRT(2.*PI))
      + *DSIGMA
       IF (SUM .GT. Z) THEN
        GOTO 90
        END IF
       ECARTTYPE = ECARTTYPE+DSIGMA
      80 CONTINUE
       END IF
      90 CONTINUE
       RETURN
       END
C     ************************************************************
       DOUBLE PRECISION FUNCTION RAND(N)
        INTEGER N,M,A,C,X0,X1
        SAVE X0
        IF (N .NE. 0) THEN
          X0=N
        END IF
        M=2**15
        A=8*INT((M/2)*ATAN(1.)*(1./8.))+5
        C=2*INT(((1./2)-SQRT(3.)/6.)*(M/2))+1
        X1=MOD((A*X0+C),M)
        X0=X1
        RAND=FLOAT(X1)/FLOAT(M)
        RETURN
       END
```

D.1 Experimental results for fermentation in the STB.

Rushton - 100 RPM									
Time (days)	Volume (m^3)	Biomass (kg/m^3)	Citric (kg/m^3)	Sucrose (kg/m^3)	Glucose (kg/m^3)	Fructose (kg/m^3)	Power (W/m^3)	PH	K_La (s^{-1})
0.01	0.0173	1.54	0.033	73.0	34.0	30.0	30	3.69	-
0.66	0.0171	2.07	0.034	19.0	62.0	43.0	28	3.47	0.00208
1.51	0.0169	2.12	0.201	0.0	74.0	65.0	28	2.94	0.00164
2.88	0.0163	2.71	0.639	0.0	69.0	67.0	28	2.66	0.00106
3.62	0.0161	2.83	0.852	0.0	74.0	70.0	30	2.61	0.00119
4.99	0.0158	3.28	1.764	0.0	74.0	70.0	31	2.54	0.00121
5.71	0.0155	4.02	2.088	0.0	74.0	69.0	31	2.52	0.00086
6.95	0.0151	4.49	2.529	0.0	77.0	73.0	32	2.44	0.00107
7.89	0.0147	4.40	3.164	0.0	70.0	66.0	34	2.43	0.00113
8.56	0.0146	4.34	3.330	0.0	74.0	69.0	35	2.38	0.00173
9.43	0.0144	5.45	3.876	0.0	78.0	71.0	37	2.38	0.00175
10.93	0.0139	5.94	4.168	0.0	84.0	75.0	37	2.34	0.00190
12.05	0.0136	5.92	4.342	0.0	80.0	70.0	38	2.29	0.00215

Rushton - 200 RPM									
Time (days)	Volume (m^3)	Biomass (kg/m^3)	Citric (kg/m^3)	Sucrose (kg/m^3)	Glucose (kg/m^3)	Fructose (kg/m^3)	Power (W/m^3)	PH	K_La (s^{-1})
0.02	0.0171	2.10	0.019	53.0	40.0	32.0	215	3.70	0.00121
0.71	0.0169	2.29	0.020	3.0	72.0	60.0	220	3.24	0.01135
1.77	0.0165	3.24	0.358	0.0	73.0	71.0	215	2.65	0.00413
2.81	0.0162	3.66	0.851	0.0	80.0	77.0	214	2.49	0.00304
3.71	0.0160	4.24	1.533	0.0	69.0	66.0	218	2.43	0.00217
4.72	0.0157	4.45	2.082	0.0	77.0	72.0	209	2.37	0.00184
5.72	0.0154	4.65	2.567	0.0	71.0	65.0	225	2.34	0.00236
7.04	0.0151	5.80	3.663	0.0	73.0	65.0	230	2.30	0.00244
7.77	0.0149	5.25	4.795	0.0	80.0	69.0	231	2.27	0.00320
8.68	0.0145	6.02	5.283	0.0	75.0	64.0	241	2.20	0.00370
9.63	0.0141	5.85	6.165	0.0	79.0	66.0	240	2.20	0.00439
10.61	0.0139	5.80	6.828	0.0	73.0	59.0	235	2.11	0.00324
11.70	0.0135	5.08	7.681	0.0	79.0	62.0	227	2.11	0.00741

Rushton - 300 RPM									
Time (days)	Volume (m^3)	Biomass (kg/m^3)	Citric (kg/m^3)	Sucrose (kg/m^3)	Glucose (kg/m^3)	Fructose (kg/m^3)	Power (W/m^3)	PH	K_La (s^{-1})
0.01	0.0175	1.97	0.032	37.0	48.5	42.5	699	3.59	0.03440
1.01	0.0175	3.27	0.036	0.0	77.0	69.5	607	2.96	0.01970
2.05	0.0171	5.63	1.219	0.0	76.0	67.5	563	2.47	0.01098
3.11	0.0169	7.79	4.200	0.0	75.0	64.0	551	2.17	0.01037
4.12	0.0165	9.95	7.406	0.0	74.0	62.0	563	2.24	0.01080
5.09	0.0165	9.67	10.000	0.0	74.0	58.0	574	2.05	0.01230
6.23	0.0163	8.74	11.606	0.0	74.0	55.5	591	1.99	0.01440
7.14	0.0161	9.68	8.781	0.0	73.5	52.0	593	1.99	0.01690
8.08	0.0160	10.57	9.756	0.0	70.5	48.5	601	1.96	0.01820
9.06	0.0158	12.66	11.281	0.0	70.5	48.5	605	1.94	0.02120
10.20	0.0155	13.68	12.844	0.0	70.0	47.0	607	1.94	0.01930
11.10	0.0154	13.97	10.419	0.0	67.5	44.5	603	1.97	0.01660
12.17	0.0153	11.12	11.963	0.0	67.0	44.5	606	2.01	0.01640

Rushton - 400 RPM						
Time (days)	Volume (m^3)	Biomass (kg/m^3)	Citric (kg/m^3)	Power (W/m^3)	PH	K_La (s^{-1})
0.03	0.0178	1.51	0.022	1508	3.58	-
1.02	0.0177	1.58	0.025	1468	2.97	0.9970
1.95	0.0171	3.78	0.932	1403	2.24	0.0239
2.99	0.0167	5.32	2.236	1366	2.02	0.0133
4.03	0.0166	6.84	3.408	1319	1.94	0.0106
5.02	0.0161	7.33	3.721	1304	1.89	0.0186
5.89	0.0159	9.36	5.600	1289	1.90	0.0179
6.86	0.0157	12.26	5.850	1296	1.93	-
7.95	0.0155	17.76	8.019	1346	1.92	0.014
8.92	0.0153	20.47	10.475	1407	1.90	-
9.99	0.0149	21.54	20.006	1237	1.90	0.01710
11.00	0.0163	19.30	16.981	1336	2.04	0.01120
11.86	0.0159	20.86	17.269	1326	2.12	0.00090

E.1 Experimental results for fermentation in the RPB.

Reciprocating - 0.25 Hz									
Time (days)	Volume (m^3)	Biomass (kg/m^3)	Citric (kg/m^3)	Sucrose (kg/m^3)	Glucose (kg/m^3)	Fructose (kg/m^3)	Power (W/m^3)	PH	K_La (s^{-1})
0.02	0.0184	2.13	0.060	49.5	45.8	42.8	143	3.60	0.00121
0.71	0.0180	2.16	0.058	15.0	74.3	53.3	143	3.46	0.00372
1.76	0.0175	2.77	0.111	0.0	75.0	73.5	141	2.56	0.00182
2.81	0.0173	6.14	0.446	0.0	74.3	68.3	165	2.17	-
3.71	0.0172	7.76	0.531	0.0	78.0	67.5	152	2.03	-
4.73	0.0169	9.73	0.683	0.0	78.0	63.8	241	1.94	-
5.73	0.0164	12.82	0.723	0.0	78.0	60.0	237	2.01	-
7.05	0.0161	14.78	0.744	0.0	78.0	59.3	242	2.24	-
7.79	0.0157	18.39	0.784	0.0	79.5	56.3	225	2.33	-
8.69	0.0152	18.76	0.922	0.0	69.8	47.3	229	2.42	-
9.64	0.0147	22.77	0.942	0.0	72.8	49.5	235	2.52	-
10.62	0.0143	23.08	1.081	0.0	70.5	45.8	240	2.55	-
11.72	0.0139	25.87	1.131	0.0	72.0	45.8	246	2.64	-

Reciprocating - 0.50 Hz						
Time (days)	Volume (m^3)	Biomass (kg/m^3)	Citric (kg/m^3)	Power (W/m^3)	PH	K_La (s^{-1})
0.02	0.0178	1.57	0.018	221	3.59	-
1.03	0.0176	1.94	0.020	221	3.02	0.00240
1.95	0.0173	3.11	0.210	230	2.29	-
2.99	0.0173	6.19	0.321	237	2.03	-
4.03	0.0171	9.03	0.373	255	1.88	-
5.02	0.0167	12.33	0.376	273	1.75	-
5.91	0.0165	11.62	0.420	269	1.84	-
6.87	0.0163	15.02	0.424	292	2.11	-
7.96	0.0163	17.52	0.529	304	2.34	-
8.94	0.0163	21.54	0.598	312	2.49	-
10.00	0.0159	23.02	0.595	323	2.71	-
11.01	0.0155	18.42	0.584	334	2.81	-
11.88	0.0171	16.33	0.772	327	2.93	-
12.76	0.0171	16.21	0.788	82	2.93	-

Reciprocating - 0.75 Hz									
Time (days)	Volume (m^3)	Biomass (kg/m^3)	Citric (kg/m^3)	Sucrose (kg/m^3)	Glucose (kg/m^3)	Fructose (kg/m^3)	Power (W/m^3)	PH	K_La (s^{-1})
0.01	0.0186	1.80	0.027	44.0	53.0	44.5	849	3.64	0.00566
0.99	0.0186	2.07	0.026	0.5	79.5	74.5	845	3.01	0.00536
2.02	0.0186	9.15	0.035	0.0	72.0	60.0	841	2.05	0.00901
3.09	0.0184	12.64	0.070	0.0	68.0	49.5	844	2.37	0.00688
4.10	0.0182	18.12	0.113	0.0	62.0	45.0	827	2.69	0.00404
5.08	0.0178	17.87	0.264	0.0	59.5	43.0	850	2.87	0.00356
6.21	0.0173	21.00	0.386	0.0	54.5	37.5	864	2.98	0.00502
7.13	0.0173	18.38	0.494	0.0	51.0	37.0	893	2.98	0.00430
8.05	0.0169	19.15	0.507	0.0	49.0	34.0	877	3.04	0.00435
9.05	0.0169	20.56	0.585	0.0	46.0	34.0	859	3.11	-
10.20	0.0167	20.48	0.648	0.0	40.5	28.5	937	3.14	0.00510
11.07	0.0166	20.50	0.649	0.0	38.0	29.5	966	3.21	0.00439
12.15	0.0163	19.64	0.632	0.0	34.0	25.5	1010	3.25	0.00429

Reciprocating - 0.1 Hz									
Time (days)	Volume (m^3)	Biomass (kg/m^3)	Citric (kg/m^3)	Sucrose (kg/m^3)	Glucose (kg/m^3)	Fructose (kg/m^3)	Power (W/m^3)	PH	K_La (s^{-1})
0.01	0.0194	1.29	-	75.0	30.0	28.0	1187	3.68	-
0.66	0.0194	2.25	0.036	14.0	73.0	45.0	1170	3.47	0.00819
1.49	0.0192	5.21	0.067	0.0	71.5	68.7	1339	2.08	0.00798
2.88	0.0182	19.70	3.038	0.0	57.0	46.0	1297	2.66	0.01060
3.62	0.0180	23.96	3.416	0.0	55.0	43.0	1255	2.66	0.00815
4.99	0.0175	23.70	3.483	0.0	48.0	39.0	1341	2.72	0.00591
5.72	0.0171	29.18	3.621	0.0	43.0	35.0	1313	2.76	0.00542

F.1 Photographs of daily samples during fermentation experiments from the STB (200 RPM) and RPB (0.25 Hz).